

Pair-instability evolution and explosions in massive stars

M. Renzo^a and N. Smith^a

^aUniversity of Arizona, Department of Astronomy & Steward Observatory, 933 N. Cherry Ave., Tucson, AZ 85721, USA

© 20xx Elsevier Ltd. All rights reserved.

(P)PISN

Glossary

pair electron (e^-) and positron (e^+) pair, also e^\pm

supernova luminous electromagnetic transient

SN Ia supernova with spectrum showing no hydrogen lines (from the explosion) but showing silicon lines

SN Ib supernova with spectrum showing helium but not hydrogen lines

SN Ic supernova with spectrum showing neither helium nor hydrogen lines

SN II supernova with spectrum showing hydrogen lines (and no silicon lines)

SN IIn SN II with narrow emission lines

SN IbN SN Ib with narrow emission lines

metallicity fraction of mass in elements heavier than hydrogen and helium

Nomenclature

SN	Supernova
SLSN	Superluminous supernova (peak absolute magnitude < 21)
PISN	Pair instability supernova
P-PISN	Pulsational pair instability supernova
BH	Black hole
GW	Gravitational wave
Z	Metallicity, that is mass fraction of elements heavier than helium
IMF	Initial mass function, that is distribution of initial masses of stars
CSM	Circumstellar material

Abstract

Very massive stars are radiation pressure dominated. Before running out of viable nuclear fuel, they can reach a thermodynamic state where electron-positron pair-production robs them of radiation support, triggering their collapse. Thermonuclear explosion(s) in the core ensue. These have long been predicted to result in either repeated episodic mass loss (pulsational pair instability), which reduces the mass available to eventually form a black hole, or, if sufficient energy is generated, the complete unbinding of all stellar material in one single explosive episode (pair instability supernova), which leaves behind no black hole. Despite theoretical agreement among modelers, the wide variety of predicted signatures and the rarity of very high-mass stellar progenitors have so far resulted in a lack of observational confirmation. Nevertheless, because of the impact of pair instability evolution on black hole masses relevant to gravitational-wave astronomy, as well as the present and upcoming expanded capabilities of time-domain astronomy and high redshift spectroscopy, interest in these explosion remains high. We review the current understanding of pair instability evolution, with particular emphasis on the known uncertainties. We also summarize the existing claimed electromagnetic counterparts and discuss prospects for future direct and indirect searches.

Key points

- Very massive, radiation pressure dominated stars encounter the pair-instability near the ends of their lives, but before they run out of nuclear fuel.
- The pair instability converts radiation energy density into rest-mass of the e^\pm pair, softening the radiation-pressure dominated equation of state and causing a collapse. Heating due to gravitational collapse triggers a thermonuclear explosion.
- In pulsational pair instability supernovae (P-PISN), the explosion causes the (possibly repeated) ejection of layers of mass, while in pair instability supernovae (PISN) it completely destroys the star, leaving no compact remnant.
- The observed light from P-PISNe is powered by the interaction between ejected shells, while the luminosity of PISNe is powered by the radioactive decay of large amount of radioactive nickel (^{56}Ni).
- Despite theoretical agreement among modelers, GW detection of BHs “in the PISN mass gap” have occurred, while the bright SNe associated with pair-instability have so far eluded detection.
- Theoretical studies continue to explore uncertainties in the input physics, stellar modeling, and interpretation of GW and electromagnetic transients. In the near future, multiple observations may help solve the apparent discrepancy between theoretical predictions and observations.

1 Introduction

The final fate of massive stars (initially $\gtrsim 7.5 M_\odot$, e.g., [Doherty et al. 2015](#); [Poelarends et al. 2017](#)) is a long-standing problem in astrophysics. For millennia (e.g., [Xi, 1955](#); [Clark and Stephenson, 1977](#); [Stephenson and Green, 2002](#); [Zhou et al., 2018](#)), we have been able to observe spectacular transients, called supernovae (SNe), which occur when a massive star’s core exhausts viable nuclear fuel. This leads to the collapse of the iron (Fe) core (or, at the lower mass end, the oxygen-neon core) under its own gravity until it “bounces” at super-nuclear densities, triggering a shock wave that *possibly* blows up the star¹. These events mark the birth of compact objects (neutron stars, NS, or black holes, BHs). Despite being routinely observed, they still pose theoretical challenges (see [Janka 2012](#); [Burrows and Vartanyan 2021](#); [Soker 2024](#) for reviews).

The situation is reversed for even more massive stars, those *ending* their lives with helium (He) core masses $M_{\text{He}} \gtrsim 50 M_\odot$, roughly corresponding to initial masses $\gtrsim 70 - 100 M_\odot$ (e.g., [Barkat et al., 1967](#); [Rakavy and Shaviv, 1967](#); [Fraley, 1968](#); [Bond et al., 1984](#); [Woosley, 2017](#)). Before running out of viable nuclear fuel, these very massive and radiation-pressure dominated stars have cores that are hot enough and have low-enough density to trigger an instability that follows from converting radiation energy density into rest-mass of electron-position pairs (e^\pm), robbing the core of some of its pressure support. This is the so called “pair instability”, which causes collapse and a thermonuclear explosion in very massive stars. There is theoretical consensus on how these stars end their lives, but unambiguous observational evidence is still lacking. The likely reasons are the intrinsic rarity of their progenitors – heavily disfavored by the stellar initial mass function (e.g., [Salpeter, 1955](#); [Kroupa, 2001](#); [Schneider et al., 2018](#)) and the large range of predicted observational signatures overlapping with other transients (e.g., [Woosley et al., 2007](#); [Woosley, 2017](#); [Smith, 2017](#); [Renzo et al., 2020b](#); [Woosley and Heger, 2021](#)). The end of the evolution of these stars is the topic of this chapter.

Interest in the final fate of these extremely massive stars is ever growing. They are thought to be the progenitors of the most massive stellar-mass BHs, bridging the gap between the stellar-mass BHs now routinely detected through gravitational waves (GW, e.g., [LVK collaboration, 2016, 2019b, 2021a, 2023a](#)), and intermediate-mass BHs ($\gtrsim 100 M_\odot$, [Mehta et al. 2022](#)). Improvements in time-domain capabilities (sky coverage, cadence, depth) are revealing rare transients that should include the death events of extremely rare very massive stars, and combined astrometric, photometric, and most importantly spectroscopic observations enable the search for nucleosynthetic signatures of the death of these stars (e.g., [Aoki et al., 2014](#); [Xing et al., 2023](#)). Finally, numerical development of stellar evolution codes has recently allowed the self-consistent exploration of the entire mass range (e.g., [Woosley et al., 2007](#); [Woosley, 2017, 2019](#); [Marchant et al., 2019](#); [Farmer et al., 2019](#); [Leung et al., 2019](#); [Renzo et al., 2020b](#); [Farag et al., 2022](#)). This has enabled new theoretical insight on the evolution of very massive stars, and has raised new questions in stellar, nuclear, and particle physics (including beyond-standard model physics).

We first review the theoretical understanding of the death of very massive stars (Section 2). We discuss the expected observational signatures (Section 3), and we summarize claims in the literature of candidates for direct detections of optical transients caused by the pair instability (Section 4). We discuss indirect evidence (Section 5), including GWs (Section 6), before highlighting the known open questions (Section 7). We conclude suggesting future prospects in Section 8.

2 Theoretical overview of pair instability

2.1 Microphysics

Here, we discuss the microphysics that determines the death of stars susceptible to the pair instability. We defer a quantitative discussion of the minimum mass needed for this process to Section 2.4. The cores of these stars experience a (potentially destructive) instability before running out of viable nuclear fuel ([Barkat et al., 1967](#); [Rakavy and Shaviv, 1967](#)), usually when the core composition is oxygen-dominated. Because of their large mass, these stars are radiation pressure dominated,

$$P_{\text{tot}} = P_{\text{gas}} + P_{\text{rad}} \simeq P_{\text{rad}} = \frac{1}{3}aT^4 , \quad (1)$$

where T is the local temperature, $a = 4\sigma/c$ is the radiation constant (σ is the Stefan-Boltzmann constant and c the speed of light). This is because virial equilibrium imposes $T \propto M$, with M total mass of the star and T average temperature, and the radiation pressure $P_{\text{rad}} \propto T^4$ grows with temperature much faster than the thermal gas pressure $P_{\text{gas}} \propto T$.

The hydrostatic evolution of these stars brings them into a thermodynamic regime where the production of electron-position pairs (e^\pm) occurs ([Breit and Wheeler, 1934](#); [Fowler and Hoyle, 1964](#)),

$$\gamma\gamma \rightarrow e^+ e^- . \quad (2)$$

Each e^\pm pair produced may then annihilate producing either a neutrino-antineutrino pair, which stream out of the star carrying away their energy, or into a pair of photons, which on average have lower energy than the original photons². This process can in principle happen in any star, since it only requires the interaction of photons with total energy in excess of the rest energy of the e^\pm pair ($E_\gamma \gtrsim 2m_e c^2$, where m_e is the electron mass). Normally, stellar interiors are in thermal equilibrium, meaning the photons follow a black-body distribution with an

¹These explosions are distinct from thermonuclear SNe, typically observed as Type Ia (e.g., [Liu et al., 2023](#), for a recent review), which correspond to the thermonuclear explosion of a white dwarf in a low-mass binary system.

²The electron or positron for the annihilation is usually not the same as the one produced in the original pair.

exponentially decaying tail at high-energy that yields a small, but non-zero, probability of having such high energy photons: pair-production alone does not necessarily result in an instability. However, when this occurs in a star whose hydrostatic equilibrium depends on radiation pressure, it can lead to a catastrophic instability: the production of e^\pm pairs effectively consumes radiation energy density. This softens the equation of state, causing a *local* thermal instability in the star. We discuss the *global* response of the star (if any) in Section 2.2.

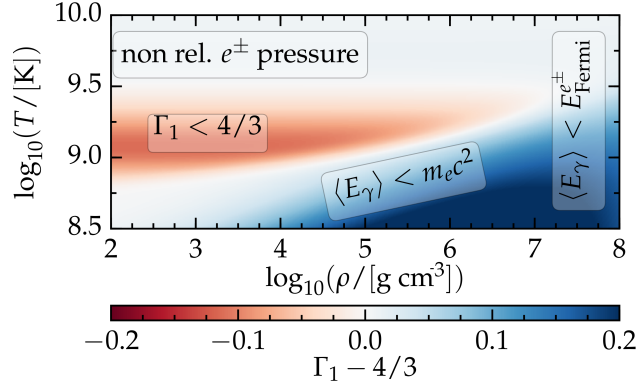


Fig. 1 First adiabatic index as a function of temperature and density for a composition typical of a PISN progenitor (mixture dominated by carbon and oxygen). In the red region $\Gamma_1 < 4/3$ resulting in a thermal instability with runaway production of e^\pm . From Renzo (2019).

Figure 1 shows first adiabatic index $\Gamma_1 = \frac{\partial \ln T}{\partial \ln \rho}|_s$ (where s is the specific entropy) on the temperature-density ($T - \rho$) plane for a composition representative of an evolved very massive star, that is mixture of carbon (C) and oxygen (O) with $\lesssim 0.1\%$ of other primordial metals. Classically, the adiabatic index Γ_1 is used to discuss the stability of a stellar structure (requiring $\Gamma_1 > 4/3$, e.g., Kippenhahn et al., 2013), and Figure 1 shows the local value of Γ_1 . Stellar layers entering the red regions, where $\Gamma_1 < 4/3$, are destabilized by the production of e^\pm pairs, which occurs around $T \gtrsim 10^9$ K corresponding to photon energies of the order of $m_e c^2 \simeq 0.511$ MeV (the pairs are produced by photons in the tail of the black body distribution). Figure 1 also annotates the microphysical mechanisms that delimit the region of local instability (see also Figure 3). At sufficiently high temperatures ($T \gtrsim 10^{9.5}$ K), the instability “chokes” itself: e^\pm pairs are produced so fast that their Fermi levels are filled, and the pairs themselves start supporting the star with their non-relativistic degeneracy pressure, bringing back $\Gamma_1 \gtrsim 4/3$ (e.g., Kippenhahn et al., 2013). Because of the energy requirement $E_\gamma \gtrsim 2m_e c^2$, pair-production is a threshold process and most e^\pm pairs are produced with negligible kinetic energy making them non-relativistic.

At sufficiently high densities $\rho \gtrsim 10^7$ g cm⁻³, the e^\pm are also degenerate (e.g., Fraley, 1968), and for pair-production to occur, the photon energy must exceed not only the rest-energy of the pair, but must also be sufficient to provide kinetic energy in excess of their Fermi energy (Zeldovich and Novikov, 1999). This extra energy requirement decreases the rate of pair production and prevents it from triggering an instability. Moreover — and possibly more importantly — at higher densities, the contribution of the gas pressure becomes increasingly important, protecting the star from catastrophic outcomes that would otherwise occur due to the drop in radiation pressure caused by pair-production. If and when lower mass stars reach inner temperatures sufficient for pair-production, the combination of these two effects prevents pair-production from triggering global instabilities.

At low temperatures, the mean photon energy is insufficient to produce pairs at rest, the precise shape of the boundary is determined by the requirement that the mean-free-path for photon-photon interactions has to be smaller than the mean-free-path for photon interactions with an electron (which are the dominant source of opacity in this regime).

2.2 Stellar evolution through pair instability

Figure 2 illustrates the phases of the stellar response to the instability described in Section 2.1 caused by the production of e^\pm pairs. Step 0 starts with a core sufficiently massive to be radiation pressure-dominated and encounter the instability, typically when its core composition is still dominated by viable nuclear fuel – C, O, possibly Silicon (Si) group elements (Marchant et al., 2019).

The instability starts at Step 1, where pair-production removes photons that were providing pressure support to the star. Because of the drop in pressure support, the star will contract. This contraction will increase its temperature, and thus also the average energy of photons in its interior $\langle E_\gamma \rangle$. Consequently the amount of photons that can do pair-production also increases. This causes a runaway production of pairs that hastens the collapse.

As the star collapses and increases its temperature, the nuclear fuel will ignite (step 3). This ignition is necessarily explosive, since the star is out of thermal equilibrium and the nuclear reaction rates are strongly temperature dependent: thus pair-instability leads to thermonuclear explosions in massive stars, and can result in three different outcomes depending on the mass of the star, which determines the ratio between the energy released by the explosive burning and the binding energy of the stellar gas.

The classical pair instability SNe (PISN, step 4a), theorized for the first time in the 1960s (e.g., Barkat et al., 1967; Rakavy and Shaviv, 1967; Fraley, 1968; Glatzel et al., 1985; Fryer et al., 2001; Woosley et al., 2007; Chatzopoulos and Wheeler, 2012; Chatzopoulos et al., 2013; Woosley, 2017; Marchant et al., 2019; Leung et al., 2019; Farmer et al., 2019; Renzo et al., 2020c,b; Farag et al., 2022; Umeda and

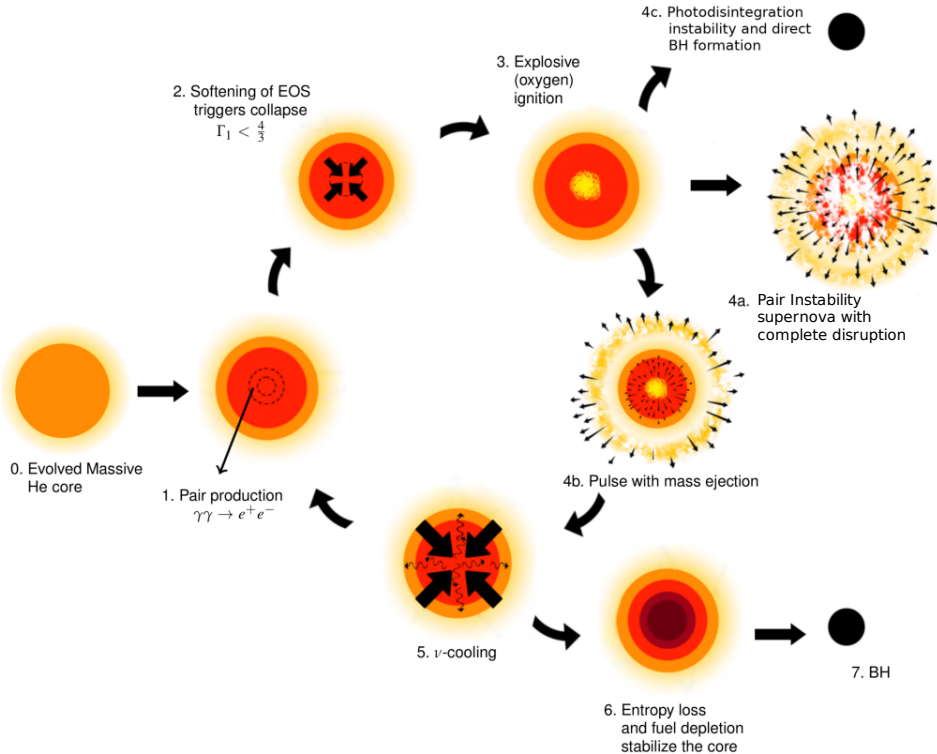


Fig. 2 Cartoon representing the core evolution through (P)PISN, from Renzo et al. (2020b). Step 4 represents the trifurcation point depending on the mass of the core: 4a represents the full disruption in a PISN occurring when the energy release by the thermonuclear explosion exceeds the binding energy of the star. For lower masses, the energy release can only unbind the outer layers, resulting in a pulse, and the cycle can repeat, producing a P-PISN (4b). For higher masses, the energy released is used to photo-disintegrate nuclei instead of accelerating gas, resulting in collapse to a BH (4c).

Nagele, 2024) occurs when the nuclear burning releases more energy than the entire binding energy of the star. In these cases, the explosions leaves no compact remnant and all the stellar material is returned to the host galaxy: PISN lead to full disruption of the star and no BH formation.

For slightly lower masses, the central temperature reached (and consequently, the nuclear burning rate) are lower: this results in less energetic explosions that fail to completely unbind the star. In these cases, the energy deposition from explosive burning triggers a pulse that propagates through the star, steepens into a shock wave as it propagates through the lower-density outer layers. This pulse may unbind some material, in a so-called pulsational pair-instability SN (P-PISN, Barkat et al. 1967; Woosley et al. 2007; Chatzopoulos and Wheeler 2012; Chatzopoulos et al. 2013; Yoshida et al. 2016; Woosley 2017; Leung et al. 2019; Marchant et al. 2019; Farmer et al. 2019, 2020; Renzo et al. 2020b,c; Farag et al. 2022), at step 4b. These are not terminal events in the life of a star, but can appear as bright transients (e.g., Woosley et al., 2007; Woosley, 2017; Lunnan et al., 2018; Gomez et al., 2019; Woosley and Smith, 2022, see also Section 3.2). Even if not unbinding the entire star, the explosion causes an expansion of the core, lowering its temperature and density and pulling it out of the instability region (cf. Figure 1). The star then relaxes on a thermal timescale, which in this regime is typically determined by neutrino cooling (e.g., Barkat et al., 1967; Fraley, 1968), although the most energetic pulses may drive the core to sufficiently low densities such that neutrino cooling is shut off, and photons (and convection) return to be the main energy carriers (e.g., Woosley, 2017; Marchant et al., 2019; Renzo et al., 2020b). This relaxation timescale can vary widely from days to 10^5 yrs (e.g., Woosley, 2017; Renzo et al., 2020b). After this relaxation phase, the star may encounter the instability again, looping through the cycle, until (i) the consumption of viable nuclear fuel at step 3, (ii) the loss of mass at step 4b, and (iii) the loss of entropy during the cooling phase at step 5 stabilize the core, making it avoid the pair-production instability. At this point, normal stellar evolution resumes, finishing to burn in hydrostatic equilibrium what nuclear fuel is left in the core, ultimately producing an Fe core-collapse event (which may or may not be associated to an electromagnetic transient). In the mass regime of interest here, it is expected that such core-collapse would result in BH formation – but its final mass is limited by the amount of mass previously lost during pulses (e.g., Woosley et al., 2002; Woosley, 2017; Marchant et al., 2019; Farmer et al., 2019, 2020; Renzo et al., 2020b; Woosley and Heger, 2021; Farag et al., 2022) and possibly in an explosion associated to the final core-collapse (though the ejecta are expected to be $\lesssim 3.5 M_\odot$, Powell et al. 2021; Rahman et al. 2022 but is, however, sensitive to uncertainties in core-collapse physics, see also Hendriks et al. 2023).

For stars even more massive than PISN progenitors, a second instability occurs, referred to as the photodisintegration instability (e.g., Bond et al., 1984; Fryer et al., 2001; Heger et al., 2003). In fact, the rate of photodisintegration, when sufficiently energetic photons are

available, scales as $\propto \rho$, while the rate of nuclear reactions dominating the energy release (initially $^{16}\text{O} + ^{16}\text{O}$, [Dessart et al. 2013](#); [Farmer et al. 2019](#)) scale like $\propto \rho^2$, and the latter can be lower than the former for sufficiently low densities. Thus, in extremely massive and thus low density stars, the energy released by the thermonuclear explosion is used to photo-disintegrate nuclei (unburned C, O, Si, and the products of the thermonuclear explosions itself). This means that all the energy is consumed to shuffle nucleons in and out of nuclei, instead of becoming bulk kinetic energy of the stellar gas in an explosion. The photodisintegration instability therefore cancels out the dynamical effect of the pair-instability, and results in the collapse of the star into a massive BH.

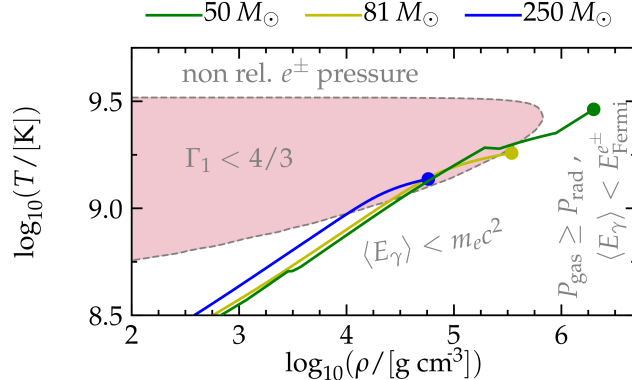


Fig. 3 $T - \rho$ profile for He cores modified from [Renzo et al. \(2020b\)](#) at the moment they approach the instability, that is when $\langle \Gamma_1 \rangle \simeq 4/3$. Models where the center is unstable ($\Gamma_{1,c} < 4/3$), experience a PISN with full disruption (yellow profile, cf. step 4a in Figure 2). Models where the center is stable ($\Gamma_{1,c} > 4/3$), experience a P-PISN (green profile, cf. step 4b in Figure 2). Extremely massive models with very low central densities ($\rho \lesssim 10^5 \text{ g cm}^{-3}$) experience the photodisintegration instability and collapse to BHs (blue profile, cf. step 4c in Figure 2). The colors label the total initial He core mass, no H envelope was included in the models of [Renzo et al. \(2020b\)](#).

Which of the three branches at step 4. a star takes is primarily determined by how much mass has low enough entropy and high enough temperature to be involved in the thermonuclear explosion, which is well approximated by the CO core mass ([Farmer et al., 2019, 2020](#)). This, in turn, is determined by the evolutionary history of the He core (e.g., [Woosley, 2019](#); [Farmer et al., 2019, 2020](#); [Renzo et al., 2020c,b](#); [Woosley and Heger, 2021](#)) and thus the initial mass of the star and its evolution, including mass loss or interaction in binaries (e.g., [Marchant et al., 2019](#); [van Son et al., 2020](#); [Laplace et al., 2021](#); [Renzo et al., 2023](#); [Hendriks et al., 2023](#); [Schneider et al., 2024](#)) and clusters (e.g., [Spera et al., 2019](#); [Di Carlo et al., 2019, 2020a,b](#); [Kremer et al., 2020](#); [Mapelli et al., 2020](#); [Costa et al., 2022](#); [Ballone et al., 2023](#)).

[Renzo et al. \(2020b\)](#) proposed a criterion to discriminate between steps 4a and 4b illustrated in Figure 3 and based on the pressure-weighted average Γ_1 ,

$$\langle \Gamma_1 \rangle = \frac{\int \Gamma_1 P d^3r}{\int P d^3r} \equiv \frac{\int \Gamma_1 \frac{P}{\rho} dm}{\int \frac{P}{\rho} dm} , \quad (3)$$

where r is the radial coordinate and m is the mass coordinate throughout the star, and the value of $\Gamma_{1,c} = \Gamma_1(r=0)$ in the center of the star. The pressure-weighting in Equation 3 is motivated by the fact that we want to predict the dynamical response of the star ([Stothers, 1999](#)), and it also naturally up-weights the high-pressure core region where the instability occurs. Stars approaching the instability ($\langle \Gamma_1 \rangle \simeq 4/3$) with a stable center ($\Gamma_{1,c} > 4/3$) experience P-PISN but finally form a BH, while stars unstable also in their center ($\Gamma_{1,c} < 4/3$) experience full disruption in a PISN. Provided a stellar profile at the onset of the instability, one can use this criterion to decide its fate without computing the dynamical phase of evolution. Models experiencing the photodisintegration instability can be identified because of their extremely low central density, needed for photodisintegrations. Nevertheless, computing the evolution of stars through P-PISN pulses (and their final core-collapse, [Powell et al. 2021](#); [Rahman et al. 2022](#)) remains necessary to determine the final BH masses.

2.3 Which stars undergo pair instability?

The processes triggered by pair-instability are all happening deep in the CO core. The mass of this CO core, as opposed to the star's initial mass, is the better metric to decide whether a star goes (P)PISN or not (e.g., [Farmer et al., 2019](#)). However, many uncertain physical processes in the evolution of massive and very massive stars (see Section 7), together with the likely occurrence of binary interactions and mergers (e.g., [Vigna-Gómez et al., 2019](#); [Di Carlo et al., 2019, 2020a,b](#); [Renzo et al., 2020a](#); [Costa et al., 2022](#); [Ballone et al., 2023](#)) make it impossible to have a robust and one-to-one mapping of initial masses with CO core masses (e.g., [Zapartas et al., 2021](#)). Consequently, any number quoted in this section is affected by large uncertainties and subject to changes as the input (e.g., nuclear reaction rates) and stellar (e.g., wind mass loss rates, convective boundary mixing) physics are updated (see Section 7).

Roughly speaking, for (P)PISN to remove significant amount of mass requires CO core masses of $M_{\text{CO}} \gtrsim 45 M_\odot$, roughly corresponding to $M_{\text{He}} \gtrsim 50 M_\odot$. These values are not the initial values, but rather the values at the time of the onset of the instability (when $\langle \Gamma_1 \rangle \lesssim 4/3$). Very roughly, stars with initial total (H-rich) masses of $\sim 70 - 100 M_\odot$ at sufficiently low metallicity may develop and retain sufficiently

massive He and CO cores to trigger (P)PISN (e.g., Woosley et al., 2002, 2007; Woosley, 2019; Yusof et al., 2013; Umeda et al., 2020; Yusof et al., 2022). Stars with lower CO core masses ($M_{\text{CO}} \gtrsim 30 M_{\odot}$) can also experience “mild” P-PISN which does not result in large mass ejections (e.g., Barkat et al., 1967; Woosley, 2017, 2019; Renzo et al., 2020b) but may still be detectable (see Section 3.1).

In terms of metallicity, because of the requirement of retaining a large He and CO core until the end of the evolution, (P)PISN is often discussed in the context of metal-free population III stars (e.g., Heger et al., 2003; Whalen et al., 2013; Umeda et al., 2020; Nagele et al., 2022). Based on hydrostatic models, Langer et al. (2007) inferred an upper-limit of $Z \lesssim Z_{\odot}/3$ for the maximum metallicity allowing for (P)PISN. This may need to be adjusted to somewhat higher metallicity, however, due to modern reductions in mass-loss rate prescriptions (e.g., Smith, 2014). This upper-limit may also be exceeded by stellar mergers producing large CO cores late in the evolution, leaving no time for the star to lose mass enough post-merger (e.g., Vigna-Gómez et al., 2019; Renzo et al., 2020a; Costa et al., 2022), or because of magnetic fields funneling back the stellar wind onto the star, preventing efficient wind mass loss (e.g., Georgy et al., 2017; Keszthelyi et al., 2019).

2.4 The theorized PISN BH mass gap

While the idea that no BHs of a certain mass would form from the collapse of stars because of PISN was already proposed in the 1960s, until the 21st century, stellar evolution calculations of the entire mass-range of interest remained challenging. This is because during P-PISN the stars experience dynamical phases of evolution (step 4b in Figure 2) with hydrostatic phases in between (steps 5-1-2 post-pulse) – two regimes that require different approximations and numerical treatments, therefore posing numerical challenges. With the exception of the closed-source code KEPLER (Weaver et al. 1978 with the relevant updates described in Woosley et al. 2002, 2007; Woosley 2017, 2019; Woosley and Heger 2021), the typical approach was to combine stellar evolution calculations (e.g., with codes such as MESA, Paxton et al. 2011, 2013, 2015, 2018, 2019; Jermyn et al. 2023 – or HOSHI, Yamada 1997) with analytic considerations or hydrodynamical calculations with a different code (e.g., FLASH, Fryxell et al. 2000 – or v1D Livne 1993) for the dynamical phase of the pulses (e.g., Chatzopoulos and Wheeler, 2012; Chatzopoulos et al., 2013; Dessart et al., 2013; Takahashi et al., 2016; Kozyreva et al., 2017; Takahashi, 2018; Umeda et al., 2020; Nagele et al., 2022; Umeda and Nagele, 2024). While this approach allows for the study of the hydrodynamics of one pulse, and is thus suitable for studying PISN, it makes it hard to follow the evolution through multiple pulses. Nevertheless, following a model through multiple pulses is needed to estimate the final, post-P-PISN, BH masses. Other stellar evolution codes (like PARSEC, see e.g., Costa et al. 2021, 2022, 2023, and GENEC, see e.g., Eggenberger et al. 2008; Yusof et al. 2013; Kozyreva et al. 2017; Yusof et al. 2022) only evolve

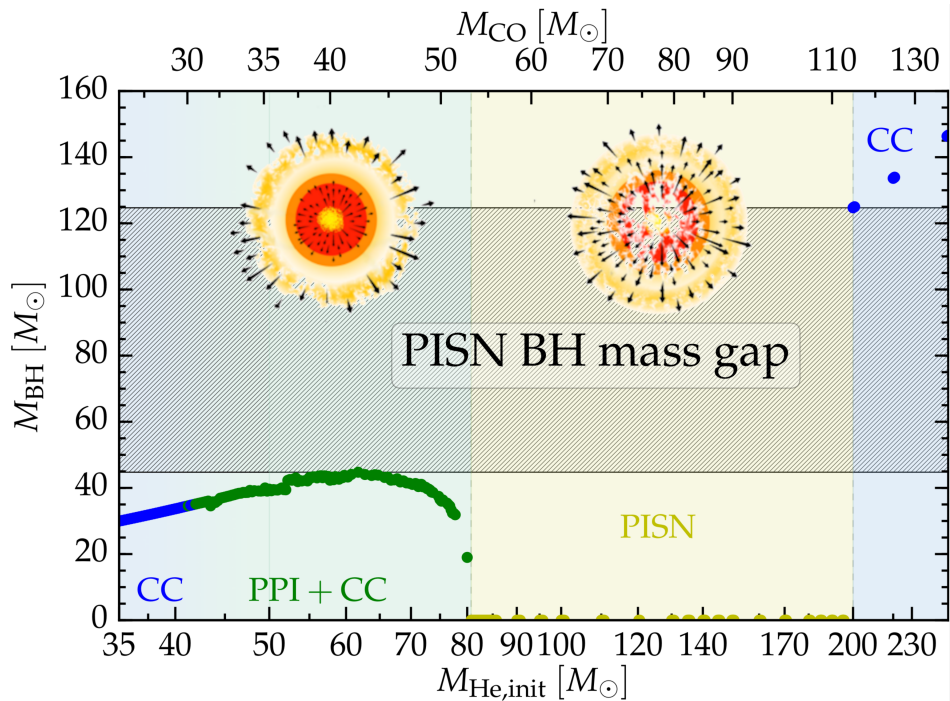


Fig. 4 Schematic illustration of the BH mass gap modified from Renzo et al. (2020b). The BH mass gap is on the y-axis (black hatch), subject to large uncertainties (see Section 7). The most up-to-date values based on the evolution of He cores are from Farag et al. (2022) and Mehta et al. (2022), with the lower edge at masses higher than $\sim 45 M_{\odot}$, which is an old value that should be disfavored based on more recent predictions – see also Figure 8 and text. The background colors indicate the predicted fate of stars: blue for core-collapse (CC), green for P-PISN followed by core-collapse (PPI+CC), yellow for PISN. The bottom x-axis shows the initial He core mass for the stellar models, and the top x-axis shows the maximum CO core mass throughout the evolution, which is a more direct parameter to determine the fate of a star. Models from Renzo et al. (2020b) only include the He core.

stellar models until core C depletion (before the pair-instability may occur) and assess the presumed fate based only on the CO core mass, predicting upper-limits for the lower-edge of the theoretical PISN BH mass gap that neglect the mass lost during P-PISN pulses.

The detection of GWs revived the interest in the BH mass gap, leading to the development of open-source and community-driven codes capable of alternating between dynamical pulses and hydrostatic phases of relaxation (e.g., Paxton et al., 2018; Leung et al., 2019; Marchant et al., 2019; Farmer et al., 2019, 2020; Renzo et al., 2020b,c; Farag et al., 2022). This enabled the exploration of theoretical uncertainties on the location of the gap (Farmer et al., 2019, 2020; Renzo et al., 2020c; Mehta et al., 2022; Farag et al., 2022), and even the inclusion of beyond-standard-model physics (see Section 7.7). The lower edge of the gap has received far more attention, partly because some estimates of its location overlap with BH masses detected through GWs, and partly because no star simultaneously sufficiently massive and metal poor to end its life above the gap is known (see also, e.g., de Koter et al. 1997; Crowther et al. 2010, 2016; Woosley 2017; Renzo et al. 2019). Predictions for GW detections further depend on the dynamical (e.g., Di Carlo et al., 2019, 2020a,b; Renzo et al., 2020a; Kremer et al., 2020; Mapelli et al., 2020) or binary interactions (e.g., Spera et al., 2019; Vigna-Gómez et al., 2019; Marchant et al., 2019; van Son et al., 2020; Hendriks et al., 2023) between the stellar progenitors of the merging BHs, which introduce further uncertainties and are under very active investigation.

Since they can cause full disruption of massive stars leaving no compact remnant, PISNe are predicted to carve a “gap” in the BH mass distribution (e.g., Rakavy and Shaviv, 1967; Fraley, 1968; Woosley et al., 2002; Chatzopoulos and Wheeler, 2012; Woosley, 2017; Takahashi, 2018; Marchant et al., 2019; Farmer et al., 2019, 2020; Renzo et al., 2020b; Woosley and Heger, 2021; Farag et al., 2022), illustrated on the y-axis of Figure 4. The lower edge of this gap is determined by total the amount of mass lost during P-PISN (which are expected to form a BH after the pulses, Woosley 2017; Renzo et al. 2020b; Powell et al. 2021; Rahman et al. 2022). Then, for the entire mass range where PISNe occur, no BHs form (yellow region in Figure 4). The upper edge of the gap is determined by the onset of the photodisintegration instability (e.g., Bond et al., 1984, see also Section 2.2), which produced massive BHs. This is sometimes referred to as the “second” mass gap, to distinguish it from the (highly debated) gap between the most massive NS and the least massive BHs (e.g., Özel et al. 2010; Farr et al. 2011, but see also e.g., Wyrzykowski and Mandel 2020; LVK collaboration 2020b).

The values on the axes of Figure 4 are subject to many uncertainties (e.g., Farmer et al., 2019, 2020; Renzo et al., 2020c; Woosley and Heger, 2021; Mehta et al., 2022; Farag et al., 2022, see also Section 7). The BH masses are estimated assuming full collapse of the matter remaining post-pulse (see also Section 7.6). The onset of P-PISN is marked by a smooth transition between the blue on the leftmost part of Figure 4 and the adjacent green region: this is because what exactly is identified as a P-PISN pulse depends on the target observable (Renzo et al., 2020b). These results are also affected by several known uncertainties in the input physics, and algorithmic representation of relevant physical processes in spherical symmetry (see Section 7).

The most updated values for the theorized location of the PISN BH mass gap (based on He core models) are from Farag et al. (2022), who found for the lower edge of the gap $\max(M_{\text{BH}}) = 69^{+34}_{-18} M_{\odot}$, and Mehta et al. (2022) who found for the upper edge of the gap $\min(M_{\text{BH}}) = 139^{+30}_{-14} M_{\odot}$ (see also Figure 8). The ranges quoted here bracket uncertainties in certain nuclear reaction rates (see also Section 7.1). These numbers are in broad agreement with the values reported by many other authors (e.g., Woosley et al., 2002; Woosley, 2017, 2019; Marchant et al., 2019; Farmer et al., 2019, 2020; Renzo et al., 2020c,b; Woosley and Heger, 2021; Farag et al., 2022), illustrating the theoretical consensus existing across authors, stellar evolution codes (KEPLER and MESA), and a variety of assumptions.

3 Observational predictions for (P)PISN

Despite being well understood from a theoretical perspective, unambiguous observational confirmation of PISN is still lacking, and the situation is even more unclear for P-PISN. This is likely due to a combination of (i) rarity of sufficiently massive and metal poor progenitors in the local universe (see Section 2.3) and (ii) variety of predictions overlapping with observed phenomenology from other transients (e.g., Woosley 2017, 2019; Renzo et al. 2020b; Woosley and Heger 2021).

3.1 What to look for?

Depending on the observable considered, one can define a P-PISN “pulse” in different ways, which impacts the range of masses that experience (P)PISN (Renzo et al., 2020b). Figure 5 shows an overview of the predicted phenomenology across a wide range of initial He core masses from Renzo et al. (2020b), discussed in more detail below.

3.1.1 Weak pulses and neutrino bursts

At the lower mass end, pulses start as oscillations in the central temperature and density (e.g., Woosley, 2017; Paxton et al., 2018; Woosley, 2019; Marchant et al., 2019; Renzo et al., 2020b). These are symptoms of *local* instability that do not trigger a *global* response and do not impact the outer layers of the star. The only potential observable of these “weak pulses” is through bursts in the neutrino (mostly from cooling) emission, which increases at every maximum of the density during the oscillations. However, because of the lack of progenitors within the horizon for current and planned neutrino detectors (e.g., Farag et al., 2020), this is not a promising detection strategy.

3.1.2 Moderate pulses and radial expansion

Increasing the core mass considered, pulses become more energetic. Before they can lead to significant mass loss ($\gtrsim 1 M_{\odot}$), there is a mass range where pulses cause significant radial expansion, but the vast majority of the mass remains bound to the star (v remains lower than the escape velocity v_{esc}). This could be observed as large amplitude photometric variations – although (P)PISN is not the only physical process

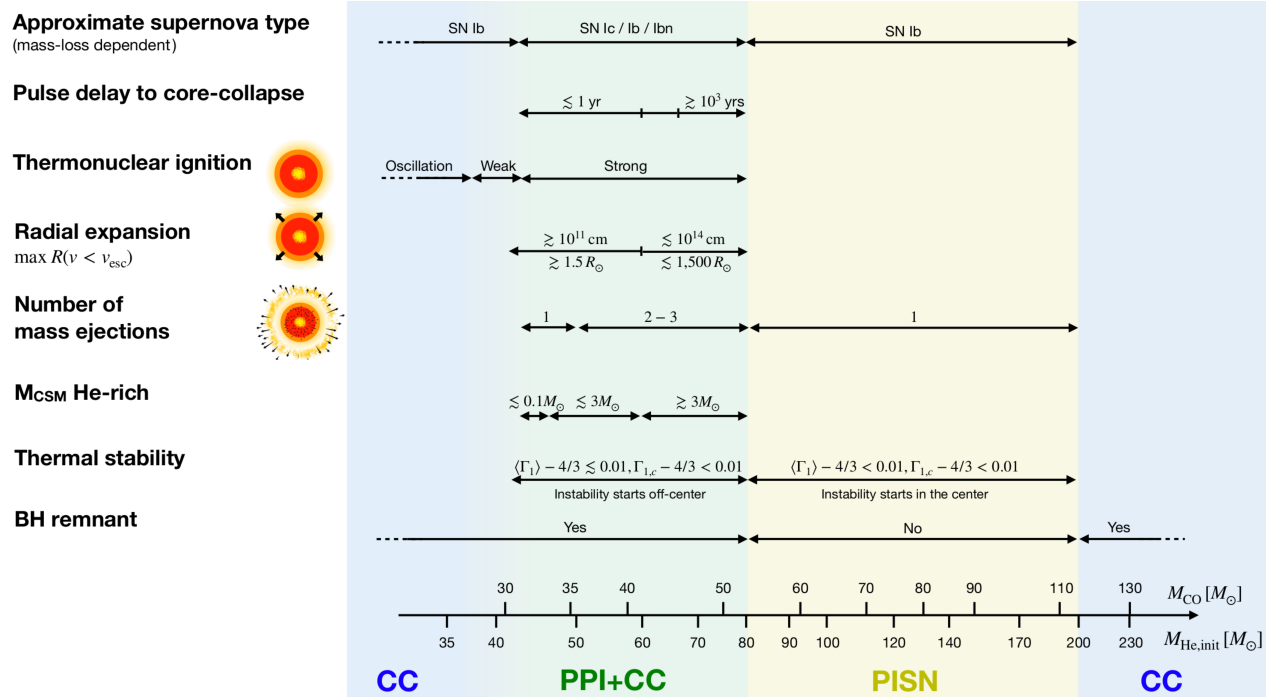


Fig. 5 Overview of (P)PISN predicted phenomenology from Renzo et al. (2020b). This overview is based on bare He cores, the background colors match those in Figure 4. M_{CSM} indicates only the He-rich circumstellar material produced, since Renzo et al. (2020b) did not include H-envelopes. The entire mass of the H-rich envelope should be added to those values in case it was retained until the first pulse (see also Section 7.6). v_{esc} indicates the local escape velocity.

that can induce those, and again the rarity of progenitors in the local Universe is a limiting factor.

Potentially more promising is the detection of the signature of binary interactions triggered by these large radius variations (e.g., Marchant et al., 2019). For example, if the companion is a compact object, large radius variations caused by P-PISN pulses could drive a high mass-transfer rate onto these, leading to copious X-ray emission. It could also induce dynamically unstable mass-transfer, although the larger the radial expansion, the lower the density of the expanded material, and the less likely these interaction would have dramatic orbital effects (Marchant et al., 2019).

3.1.3 Strong pulses and mass loss

Moving further up in CO core mass, P-PISN start removing large amount of mass, and eventually full-disruption by PISN removes *all* the mass, leaving no compact remnant behind. This is the regime that has received most attention historically (e.g., Barkat et al., 1967; Fraley, 1968). The precise amount of mass loss and the shape of the $M_{\text{BH}}\text{-to-}M_{\text{CO}}$ map are still actively being studied (e.g., Woosley, 2017; Renzo et al., 2020c,b; Mehta et al., 2022; Farag et al., 2022; Renzo et al., 2022; Hendriks et al., 2023) and is known to be sensitive to nuclear reaction rates (e.g., Takahashi, 2018; Farmer et al., 2019, 2020; Mehta et al., 2022; Farag et al., 2022, see also Section 7.1) and the numerical resolution (e.g., Farmer et al., 2019; Farag et al., 2022).

Overall, more massive cores experience more violent instabilities, producing stronger thermonuclear explosions and more mass loss (Woosley et al., 2007; Woosley, 2017; Marchant et al., 2019; Farmer et al., 2019, 2020; Renzo et al., 2020b, 2022; Farag et al., 2022); within the mass-range for strong pulses (see Section 2.3) the lowest mass BHs come from the initially more massive cores which experience more mass loss. However, there is a minimum BH mass that can be reached. Marchant et al. (2019) calculated that cores capable of losing sufficient mass to drop their total mass below $\sim 10 M_{\odot}$ would also produce sufficient amount of ^{56}Ni that the remaining $\sim 10 M_{\odot}$ of mass would be unbound by the decay of this isotope³.

To determine the number of mass-ejection events in strong P-PISN, that is, how many times a star goes through the loop in Figure 2 stellar evolution codes need to carefully define the mass ejection events. Renzo et al. (2020b) and Umeda et al. (2020) both found with completely independent computational approaches that the number of distinct mass-ejection events (step 4b in Figure 2) is $\lesssim 3$. The time-delay in between pulses, determined by the timescale for the post-pulse relaxation (step 5 in Figure 2) is a strong function of the CO core mass, as Figure 6 shows. More massive cores that experience stronger pulses are also driven farther from equilibrium and take a longer time to relax. At the most massive end, the delay time between core-collapse and the end of a mass-ejecting pulses $t_{\text{CC}} - t_{\text{pulse end}}$ reaches

³We note however that Marchant et al. (2019) models employed a small nuclear reaction network, known to introduce large uncertainties in the ^{56}Ni yields, see also Farmer et al. (2016, 2019); Renzo et al. (2020b).

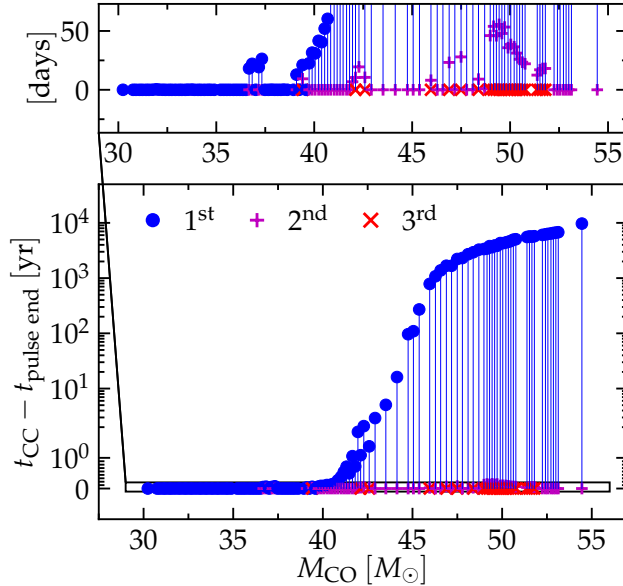


Fig. 6 Time delay between dynamically distinct mass ejection events from Renzo et al. (2020b). At the low-mass end, many stars result in delay times of months, potentially creating (He-rich) circumstellar material detectable with flash spectroscopy.

$\sim 10^5$ yr, that is roughly the Kelvin-Helmholtz timescale of stars of this mass accounting only for their photon luminosity. This is because the pulse expanded their core to the point where neutrino cooling emission shuts off. Conversely, at the low mass end, many interpulse time of weeks to months can be found: this can lead to bright transients if subsequent pulses collide with each other (e.g., Woosley et al., 2007; Woosley, 2017; Renzo et al., 2020b) or if the final core-collapse (CC) event produces an outflow.

Within each strong pulse, the ejecta have some velocity structure, but overall the velocity is comparable to the escape velocity from the surface ($v_{\text{esc}} \simeq 10 - 100 \text{ km s}^{-1}$ for red supergiants and $\simeq 1000 \text{ km s}^{-1}$ for blue and/or stripped progenitors). This can produce faster ejecta in the second and third pulse (especially if the first pulse occurred in an expanded red supergiant, while the second and third occur from a now stripped and much more compact star), leading to collisions and electromagnetic signals powered by conversion of kinetic energy into radiation (e.g., Woosley et al., 2007; Woosley, 2017, 2019; Renzo et al., 2020b).

3.2 Electromagnetic transients

3.2.1 Pulsational pair instability supernovae: collision of circumstellar shells

As discussed in Section 3.1, strong pulses can produce a wide range of mass loss amount and timing, and power transients by converting kinetic energy of the ejecta into radiation. This causes the wide range of predictions for (P)PISN transients and consequently the difficulty in finding non-controversial observational candidates. Some are brief events (essentially a series of closely spaced pulses that merge together) with irregular light curves, and some have repeating events spread over many years.

Matter ejected in a pulse can have a velocity structure (e.g., Woosley, 2017; Renzo et al., 2020b), leading to internal collisions, but most importantly, the 2nd and 3rd dynamically distinct ejection events can come from deeper in the potential well of the star, that is with higher $v \simeq v_{\text{esc}}$ compared to the first ejection. This allows them to catch up with the first pulse, producing a non-terminal event of comparable luminosity as a terminal SN explosion by converting kinetic energy of the gas into radiation. In this sense, P-PISN have some overlap with SNe of Types IIn and Ibn (Smith, 2017), but with different expected velocities seen in spectra. This may even produce super-luminous events, but this is not necessary: many P-PISN don't reach absolute magnitudes below -21 (Woosley, 2017; Kozyreva et al., 2017). Woosley et al. (2007) and Woosley (2017) calculated with KEPLER light curves for P-PISN showcasing the wide phenomenology that theory predicts. Nevertheless, specific trends in mass are expected, as exemplified in Figure 6 for the time delay between the pulses and final collapse, and may become testable in the future (Renzo et al., 2020b).

We emphasize that if the final collapse produces some, even weak, outflow (e.g., Kuroda et al., 2018; Burrows et al., 2023; Powell et al., 2021; Rahman et al., 2022), the final blast wave can also potentially interact with previously ejected shells, leading after "SN impostor" events to a final terminal transient (e.g., Woosley and Smith, 2022).

In another chapter in this Encyclopedia, Dessart (2024) reviewed interaction-powered SNe, of which P-PISN may represent an extreme case (in terms of progenitors and mass in the circumstellar shells).

3.2.2 Pair instability supernovae: radioactive power

The situation is less varied for PISNe, expected to be singular events that obliterate the star in only one pulse (step 4a in Figure 2), leaving no compact remnant. These are thermonuclear SN powered by radioactive decay from a large synthesized mass of ^{56}Ni buried inside a

large mass of stellar ejecta. The mass of ^{56}Ni synthesized can exceed by orders of magnitude the production of this isotope in core-collapse SNe. This result in very high luminosity transients (up to $\sim 10^{44}$ erg s $^{-1}$, [Kasen et al. 2011](#)). However, the range of ^{56}Ni masses spans $\sim 0.05 - 60 M_{\odot}$ (e.g., [Woosley et al., 2007](#); [Farmer et al., 2019](#); [Renzo et al., 2020b](#)) so not all PISN are necessarily super-luminous SNe (e.g., [Kozyreva et al., 2017](#)). In fact, the more massive the progenitor CO core, the higher the synthesized ^{56}Ni mass (e.g., [Woosley, 2017](#); [Renzo et al., 2020b](#)), so assuming the CO core mass scales with the initial total mass, the initial mass function (IMF) disfavors super-luminous PISNe.

H-rich PISN are expected to have long-lasting light curves determined by long radiation diffusion timescale across the ejecta ([Kasen et al., 2011](#); [Dessart et al., 2013](#); [Kozyreva et al., 2017](#)). H-poor transient instead do not necessarily have large opaque ejecta masses, and fast and bright transient may be produced ([Kozyreva et al., 2017](#)). In both cases, the light curves are expected to be smooth (no prior eruptions pollute the circumstellar environment).

4 Observed transients

Several transient surveys are searching the sky for SNe and other types of time variable phenomena, and it is obviously interesting to consider whether transients triggered by the pair instability are among the observed population of transient sources being detected in these surveys. The intrinsic rate of pair-instability transients should be rare compared to normal SNe, because of the slope of the IMF. However, at extremely low metallicity, the IMF may be skewed to higher masses because of inefficient cooling during star formation (e.g., [Zinnecker and Yorke, 2007](#)), and stellar winds are weaker, possibly making (P)PISN more common. Thus, it has long been hoped that *JWST* might be able to see signs of PISNe from Pop III stars at very high redshift (e.g., [Whalen et al., 2013](#); [Regos et al., 2020](#)).

On the other hand, recent decades have seen significant reductions in empirical estimates of line-driven wind mass-loss rates for hot stars ([Smith, 2014](#)). In addition, untargeted transient surveys have found many examples of unusual luminous transients, often in very faint (presumably low-metallicity) host galaxies, and observers have sometimes appealed to pair instability events for the unusual observed explosions. In this section we review some of the transients for which the pair instability has been invoked as a potential explanation.

From an observational perspective, it is useful to discuss true PISNe and P-PISNe separately, as the expected transients are very different beasts, despite arising from the same trigger mechanism (e.g., [Woosley, 2017](#)). Below we discuss a number of events for which the PI was suggested as a potential cause, and we comment on how well they agree with expectations for PISNe and P-PISNe. Lists of candidate events have also been compiled in [Renzo et al. \(2020b\)](#) (focused on H-poor events) and [Hendriks et al. \(2023\)](#).

4.1 PISN candidates

SN 2006gy: This was the first recognized super-luminous” supernova (SLSN). In addition to a very high peak luminosity, it had a slowly rising, smooth light curve, and a PISN was suggested as one possible explanation for its origin ([Smith et al., 2007](#)); although interaction with a massive shell of circumstellar material (CSM) produced by a massive star eruption was considered more likely ([Smith and McCray, 2007](#); [Smith et al., 2007](#)). SN 2006gy was a Type IIn event, indicating that it had narrow H emission lines from H-rich CSM. In its late-time decline, SN 2006gy faded too quickly as compared to the sustained radioactive decay tail that would have been expected from the large mass of ^{56}Ni powering the main peak in the PISN hypothesis ([Smith et al., 2008](#); [Miller et al., 2010](#)). This disfavored the PISN hypothesis, although the P-PISN was a suggestion for the origin of the strong CSM interaction (see Section 4.2).

SLSNe Ic: Around the same time SN 2006gy was being interpreted, another class of SLSNe emerged, which had H- and He-poor spectra (hence, classified as Type Ic-like spectra) and lacked the narrow lines from CSM ([Quimby et al., 2011](#)), with SN 2005ap being the prototype ([Quimby et al., 2007](#)). The situation with PISNe and this class is very reminiscent of SN 2006gy above: although the PISN hypothesis was initially discussed because of their high peak luminosity and smooth lightcurves, they fade too quickly at late times to be explained by radioactive decay from a large mass of ^{56}Ni , and thus, true PISN was rejected as an explanation ([Quimby et al., 2011](#)). The currently favored explanation is a H-free core-collapse SN that has added power from magnetar spin-down ([Woosley, 2010](#); [Kasen and Bildsten, 2010](#)), and CSM interaction via a P-PISN (see Section 4.2) may also be viable.

SN2007bi: This was a H-poor SLSN, similar in some respects to the SLSNe Ic discussed above. Unlike those objects, however, it faded at a slower rate that was consistent with radioactive decay from a large mass of ^{56}Ni , and was proposed to be a true PISN ([Gal-Yam et al., 2009](#)). However, spectral synthesis models predicted that true PISNe will be quite red and cool because of strong line blanketing from the large synthesized mass of Fe-group elements, whereas SN 2007bi was very blue, disfavoring the PISN hypothesis ([Dessart et al., 2013](#); [Moriya et al., 2019](#)). These models also predicted more slowly evolving light curves than SN 2007bi. Instead, CSM interaction appears to be a viable explanation for SN 2007bi ([Moriya et al., 2010, 2019](#)).

SN2018ibb: Recently, [Schulze et al. \(2024\)](#) described long ($\gtrsim 1000$ days) photometric and spectroscopic followup of this H-poor SLSN, and proposed it as a very strong PISN candidate based on its slowly evolving light curve and spectrum, months-long rise time, relatively slow ejecta velocities (from Fe II lines), peak bolometric luminosity $\gtrsim 10^{44}$ erg s $^{-1}$ corresponding to a radiated energy $E_{\text{rad}} \gtrsim 10^{51}$ erg. The transient has sufficiently faded to detect the host dwarf galaxy with metallicity $\sim Z_{\odot}/4$. These observations are all in agreement with theoretical prediction for PISN from very massive stars producing tens of solar masses of ^{56}Ni , making it one of the best candidates to date. However, this transient also showed cobalt lines – unexpected because of line blocking in PISN models, and evidence for CSM interaction and a blue excess. The presence of CSM is not naturally explained by PISN models, although it should be noted that the theoretically unexpected presence of CSM occurs in many non-exotic SNe as well (cf. [Dessart \(2024\)](#) chapter of this encyclopedia).

4.2 P-PISN candidates

As discussed above, P-PISN should arise from a range of initial masses that is lower than the mass range giving rise to true PISNe, and thus, we might expect P-PISNe to be somewhat more likely among the observed transient population. On the other hand, the possible observed outcomes of multiple shell collisions from P-PISNe are more diverse than for PISNe (Woosley, 2017), perhaps making them harder to differentiate from other CSM interaction transients. Below, we mention some examples discussed in the literature.

SN 2006gy: In addition to being the first proposed example of a true PISN, SN 2006gy was also suggested as a possible example of a P-PISN (Woosley et al., 2007; Smith et al., 2010a), due to its high luminosity, slow evolution, and observational signatures of strong CSM interaction. Its massive inferred CSM shell ($\sim 20 M_{\odot}$; Smith and McCray 2007; Woosley et al. 2007) ejected only a decade before discovery (Smith et al., 2010a) cannot be explained by any stellar wind scenario, but could have arisen from a previous pair pulsation that ejected much of the H envelope. The mass and energy budgets, as well as the approximate appearance of the lightcurve (with some caveats), are plausibly accounted for with a P-PISN model (Woosley et al., 2007). SN 2006gy was a Type IIn event, meaning that it had narrow lines from slow H-rich CSM. In most cases, the first pulse is the most energetic (Woosley, 2017; Renzo et al., 2020b), typically removing the remaining H envelope (if any is left, see also Section 7.6) in an explosive blast with bulk expansion speeds of a few thousand km s^{-1} (Woosley, 2017; Renzo et al., 2020b; Woosley and Smith, 2022). However, in some models of P-PISNe for SN 2006gy with long delay times between pulses, slower CSM speeds of $\sim 200 \text{ km s}^{-1}$ are seen initially, with the observed pre-shock velocities rising as the SN fades. This is in quite good agreement with spectra of SN 2006gy, which showed pre-shock CSM expansion speeds of a few hundred km s^{-1} , rising with time as the shock expanded outward as if running through a self-similar flow rather than a steady wind (Smith et al., 2010a). Overall, the P-PISN mechanism appears to give a good explanation for SN 2006gy, although a predicted very bright precursor event was not detected, and other mechanisms for pre-SN mass loss are not ruled out.

SN2009ip: This was a Type IIn supernova observed in 2012 (Mauerhan et al., 2013), but before its final SN event it was seen as a very luminous and likely very massive progenitor that had a series of non-terminal LBV-like precursor outbursts (Smith et al., 2010b). Based on its precursor outbursts and strong CSM interaction in the spectrum, plus an integrated radiated energy of only $\sim 10^{50} \text{ erg}$, a P-PISN was one proposed scenario for this object (Fraser et al., 2013; Pastorello et al., 2013). However, significant asymmetry inferred from polarization and other observed properties indicated instead that the 2012 event was a 10^{51} erg explosion that was typical for a core-collapse SN from a blue supergiant (Mauerhan et al., 2014; Smith et al., 2014). Moreover, the broad-line spectrum of the underlying SN ejecta (i.e. “underneath” the narrow H lines) was nearly identical to that of SN 1987A at many phases, showing broad H P Cygni profiles that indicated a large mass of H-rich ejecta (Smith et al., 2014). As noted above for SNe IIn in general, retaining a massive H envelope even after a series of major pulses is inconsistent with a P-PISN for this object.

iPTF14hls: This object was dubbed “The Impossible Supernova” (Arcavi et al., 2017), due to its high-luminosity multi-peaked light curve that persisted for over 600 d while its spectrum hardly changed at all. It also had a detected precursor eruption in the 1950s. A P-PISN would potentially account for the mass budget and multiple eruptions (Vigna-Gómez et al., 2019; Wang et al., 2022), but as Arcavi et al. (2017) noted, the presence of H lines in the ejecta were problematic for a P-PISN, similar to the cases of SN 2009ip and normal SNe IIn as discussed below. Later spectra revealed narrow emission and double-peaked intermediate-width emission, which were interpreted as a toroidal CSM interaction region that was overtaken by the ejecta, powering the sustained luminosity from within (Andrews and Smith, 2018). These authors noted that pre-SN binary interaction (Smith and Arnett, 2014) would be a plausible explanation for the origin of the asymmetric CSM, rather than a P-PISN.

SN 1961V: This has always been considered a very enigmatic explosion. Together, η Car and SN 1961V comprised Zwicky (1964)’s oddball class of “Type V” supernovae, although it would likely have been classified as Type IIn had that designation existed at the time (Smith et al., 2011a). SN 1961V had a very irregularly shaped, slowly evolving light curve and somewhat narrow emission lines suggesting expansion speeds of $2000\text{--}3700 \text{ km s}^{-1}$ (Bertola, 1963; Zwicky, 1964; Branch and Greenstein, 1971). It also had a very luminous progenitor star that was detected decades before the SN, which resided in a giant H II region and was estimated to have a very high initial mass of $M_{\text{ZAMS}} \approx 240 M_{\odot}$ (Goodrich et al., 1989), although this initial mass may be lower because of revised extinction, distance estimates, and/or the presence of undetected companions. Although its vague similarity to the eruption of η Car led it to be considered as an LBV or supernova impostor (Goodrich et al., 1989; Filippenko et al., 1995; Humphreys et al., 1999), its peak luminosity was much brighter than any other SN impostor and seems to have more in common with SNe IIn (Smith et al., 2011a). Comparing the observed progenitor, historical lightcurve, late-time flux, and reported velocities to model expectations, Woosley and Smith (2022) found that P-PISN events from $100\text{--}115 M_{\odot}$ progenitors give an excellent match to all available data. Importantly, P-PISN models that best matched the light curve also had progenitor stars with the approximately the correct luminosity. Altogether, Woosley and Smith (2022) concluded that SN 1961V was very likely a P-PISN, and is difficult to explain with any other explosion mechanism.

Other SLSNe IIn and SNe IIn: In general, SNe IIn and especially SLSNe IIn require extreme pre-SN mass loss that is difficult to explain with steady stellar winds (see Smith, 2017, for a review of interacting SNe). As a result, the P-PISN is often cited as a possible mechanism to create the dense CSM. While SLSNe IIn are admittedly quite rare, regular SNe IIn are far too common (roughly 8–9 % of all core-collapse SNe; Smith et al. 2011a) to all be caused by the P-PISN, which are limited to the most massive stars, and should be <1% of the core-collapse SN rate. While it is difficult to rule out any individual event on these grounds alone, we can be confident, based on rates, that the vast majority of SNe IIn do not arise from P-PISNe. Most SNe IIn and SLSNe IIn have the difficulty that their CSM is consistently too slow, with CSM expansion speeds typically around $80\text{--}200 \text{ km s}^{-1}$, and generally not showing increases in speed indicative of a self-similar flow in the CSM. Moreover, in many cases, spectra of SNe IIn and SLSNe IIn show broad H emission lines from the unshocked SN ejecta during the decline from peak (refs). This is at odds with the P-PISN mechanism, since the first pulse is expected to be the most energetic and should easily remove the remaining H envelope. This means that the subsequent fast SN ejecta that are overtaking any CSM should be

H-free in a P-PISN. This probably rules out the P-PISN mechanism for most SNe IIn and SLSNe IIn (Woosley and Smith, 2022; Smith et al., 2024).

Transients compatible with P-PISN predictions have also been claimed among the H-free SNe, too many to provide a complete list here. Below we highlight some of the most notable candidates.

SN 2010mb: This was a H- and He-free transient (type Ic) showing large ejecta masses and a long decay inconsistent with radioactive decay (e.g., Ben-Ami et al., 2014). Spectroscopic signatures indicated the presence of a dense and slow moving CSM, suggesting that the progenitor had shed mass from the CO core – making P-PISN the leading model to explain this transient (Ben-Ami et al., 2014).

SN 2006jc: This was a Type Ibn supernova that was interacting with He-rich/H-poor CSM. Although it was not an extraordinarily luminous event, a P-PISN was mentioned as a possible origin for the CSM based on the fact that it had a detected precursor outburst 2 yr before the SN was discovered (Pastorello et al., 2007; Yoshida et al., 2016). If this were a P-PISN, the star must have lost most of its H previously in its evolution. The mass and energy budget would have been on the low end for P-PISN models, implying a He core mass of 30-40 M_{\odot} (Woosley, 2017), although models in that range also predict a large number of weak rapid pulses, rather than only 2 pulses separated by 2 yr (i.e., longer delays between pulses of years correlate with larger ejecta masses and larger pulse energies than observed estimates for SN 2006jc). Nevertheless, the sensitivity of these predictions to stellar evolution uncertainties (see Section 7) makes a P-PISN interpretation still possible.

iPTF16eh: Lunan et al. (2018) studied this SLSN and detected through light echoes the presence of a O-rich CSM shell compatible with the ejection of core-material by a previous P-PISN pulse.

SN 2016iet: Gomez et al. (2019) interpreted this event as the final explosion of a CO core embedded in H-poor CSM produced by previous P-PISN pulses. While the timing inferred for the pulse (\sim decade prior to the SN detection) fits, the amount of H-poor CSM mass required for the lightcurve is challenging to reconcile with existing P-PISN models and the total mass of the expected progenitors.

5 Indirect evidence

Direct, unambiguous detection of transients interpreted as (P)PISN have been challenging, thus many authors have focused on indirect searches based on the signatures (P)PISN may leave in stars formed from their ejecta and/or integrated signal of distant sources. Any indirect evidence for very massive stars in the early universe or at very low metallicity (top heavy initial mass function – e.g., Schneider et al. 2018, super-massive BH formation from direct collapse of supermassive stars – e.g., Greene et al. 2020, diffuse X-ray background – e.g., Sartorio et al. 2023, etc.) can also be used to support indirectly the occurrence of these explosions, but definitive conclusions are still lacking.

One clear predicted signature is in the nucleosynthesis of these explosions. For P-PISNe most of the ejecta will come from the H-rich envelope (if any, see Section 7.6), the He core, and possibly outer-layers of the CO core – except for (poorly understood, cf. Section 7.2) mixing during the pulse propagation, these are unlikely to eject much newly synthesized material. Conversely, PISNe return all of their material to the host galaxy ISM, and a larger fraction of the ejecta will be nuclear processed material synthesized in the explosion (e.g., Woosley et al., 2002; Takahashi et al., 2016; Takahashi, 2018; Farmer et al., 2019). Since these explosions occur in a hot, and low density CO core without free neutrons, this is expected to produce a specific pattern in the nuclear yields: neutron-rich isotopes with odd number of nucleons (which would require more neutrons) are highly disfavored, resulting in a characteristic “odd-even” pattern in the yields (e.g., Truran and Arnett, 1970; Woosley et al., 2002; Takahashi, 2018). We emphasize that while the composition and temperature of the thermonuclear explosions in white-dwarfs powering SNIa are similar to those in (P)PISN, the density is much higher in the former leading to electron captures and formation of neutron-rich isotopes that prevent a strong odd-even effect in thermonuclear explosions of white dwarfs (e.g., Gronow et al., 2021, and references therein).

The characteristic lack of “odd elements” with a neutron excess may be detectable in the composition of the next-generation stars formed from the gas enriched by PISN. So far, unambiguous detections are lacking. Traditional searches have focused on the spectroscopic analysis of very low metallicity stars in the galactic halo, and have produced several claimed detections (e.g., Aoki et al., 2014; Xing et al., 2023). However, these remain controversial and potentially explainable invoking only core-collapse SN yields (e.g., Takahashi, 2018; Thibodeaux et al., 2024). In general, only nuclear yields from KEPLER models Woosley et al. (2002, 2007); Woosley (2017, 2019) are available for these analyses, which makes them vulnerable to unquantified systematic uncertainties. Moreover, the focus on metal-poor low mass stars may actually cut out candidate stars, if between the PISN explosions and the formation of descendant stars, CCSNe can also pollute the interstellar material, diluting the nucleosynthetic signature of PISN.

6 The gravitational-wave window

The direct detection of GW from the coalescence and merger of binary BHs opened a new way to study the distribution of remnants from massive star evolution. Because (P)PISN can decrease the mass of BHs resulting from the evolution of stars (due to mass-loss during the pulses, step 4b in Figure 2) and/or prevent BH formation completely (in the case of full PISN, step 4a in Figure 2), the direct detection of GW has revived the interest in these explosions (e.g., Woosley, 2017; Spera and Mapelli, 2017; Talbot and Thrane, 2018; Marchant et al., 2019; Stevenson et al., 2019, see also Section 2.4 and references therein) and the potential signature they may imprint on the BH mass distribution, which could also be a “standardizable siren” for cosmological applications (e.g., Farr et al., 2019).

However, less than a decade after the first direct detection of a GW merger (LVK collaboration, 2016) and with ~ 100 binary BH

detected to date (LVK collaboration, 2023a), a clear signature of (P)PISN in GWs is also lacking. Figure 7 shows the bias-corrected binary BH merger rate inferred in LVK collaboration (2023b) as a function of the mass of the most massive BH in the merging binary m_1 . Figure 7 shows a tail extending to $\sim 90 M_\odot$ and a feature for BH masses of $\sim 35 M_\odot$. While this figure shows a parametric (powerlaw + gaussian) model where such a feature is forced to be a peak, that a feature around $\sim 35 M_\odot$ exist is robustly found with different parametric models (e.g., LVK collaboration, 2021b; Edelman et al., 2021) and non-parametric analyses (e.g., Ray et al., 2023; Callister and Farr, 2024).

While several studies predicted a pile-up of BHs at the bottom edge of the theorized PISN BH mass gap because of mass loss from P-PISN (e.g., Woosley, 2017; Spera and Mapelli, 2017; Talbot and Thrane, 2018; Stevenson et al., 2019; Marchant et al., 2019; Farmer et al., 2019, 2020; Renzo et al., 2020b, 2022; Farag et al., 2022), $\sim 35 M_\odot$ is much lower than predictions from stellar evolution models (e.g., Woosley, 2017, 2019; Marchant et al., 2019; Farmer et al., 2019, 2020; Renzo et al., 2020b; Mehta et al., 2022; Farag et al., 2022; Hendriks et al., 2023).

In Section 7 we review the known uncertainties that could affect stellar evolution predictions, and although these may allow for moving the predicted lower edge of the PISN BH mass gap as low as $35 M_\odot$, this cannot be done without introducing some tension elsewhere. For example, increasing the rate of certain nuclear reaction rates (namely, $^{12}\text{C}(\alpha, \gamma)^{16}\text{O}$, see Section 7.1 and Takahashi 2018; Farmer et al. 2020; Costa et al. 2021; Mehta et al. 2022; Farag et al. 2022; Hendriks et al. 2023; Croon and Sakstein 2023b; Golomb et al. 2023) can put the lower edge of the PISN BH mass gap at $\sim 40 M_\odot$ (see Figure 8, and Farmer et al. 2020; Mehta et al. 2022; Farag et al. 2022). However, this would require a variation of more than 3σ in this rate, in tension with recent nuclear laboratory measurements of this reaction (e.g., deBoer et al., 2017; Shen et al., 2023). Moreover, shifting to lower (CO core) masses the PISN BH mass gap causes an increase in the predicted rate of (P)PISN (because of the increased probability of forming sufficiently massive cores according to a stellar initial mass function), and thus increasing the tension with the scarcity or lack of transients robustly identified as (P)PISN (e.g., Hendriks et al., 2023). For these reasons, several studies have disfavored the interpretation of the feature at $\sim 35 M_\odot$ as a signature of (P)PISN (e.g., Hendriks et al., 2023; Golomb et al., 2023; Briel et al., 2023) and alternative explanation are currently highly debated.

Figure 7 also shows a tail of BH masses extending all the way to $\sim 90 M_\odot$. We discuss in Section 7 (and specifically in Section 7.6) systematic uncertainties in stellar models that may lead to such BH masses, although again it is hard to reconcile those without creating some tension elsewhere. Moreover, several individual GW events showed at least one BH in the predicted gap (if not both, e.g., for GW190521, LVK collaboration 2020a although see also Fishbach and Holz 2020) seem to be at odds with the predictions on (P)PISN. As we discuss in Section 7.5, accretion onto the first-born BH cannot explain these events: it would need to be highly super-Eddington, and most importantly, it would result in significant orbital widening, preventing GW-driven inspiral and merger within the age of the Universe (van Son et al., 2020). These very massive BHs could be reconciled if the PISN BH mass gap moves towards higher (CO core) masses – helping also with the lack of electromagnetic detections of (P)PISN – which could happen because of several reasons from changes in the input nuclear reaction rates (e.g., Takahashi, 2018; Farmer et al., 2020; Farag et al., 2022; Mehta et al., 2022, and Section 7.1), treatment of convection and boundary mixing (e.g., Farmer et al., 2019; Renzo et al., 2020c; Umeda et al., 2020, and Section 7.2), or the fate of the H-rich envelope for models just below the threshold for (P)PISN (e.g., Vink et al., 2021; Sabahit et al., 2023; Winch et al., 2024, see also Section 7.6). Another potential explanation proposed by Shibata et al. (2021) is that the signal from these events may not be due to a binary BH merger in the first place (although see Siegel et al. 2022). Mass-loss at BH formation post P-PISN, usually not accounted for in stellar evolution simulations (Renzo et al., 2022), could remove mass in BHs forming above the gap (step 4c in Figure 2) polluting the gap “from above” (Siegel et al., 2022). Finally, there is the possibility that these events come from dynamical channels and involve 2nd (or higher) generation BHs which are not direct products of stellar evolution (e.g., Romero-Shaw et al., 2020).

Figure 7 also shows how the inferred merger rate as a function of BH mass is still changing (from the second to third catalog published), and the mass estimates for each individual event are sensitive to the priors assumed in the analysis (Fishbach and Holz 2020). One should expect further surprises as ground-based GW observations continue and space-based GW observation start in the next decade.

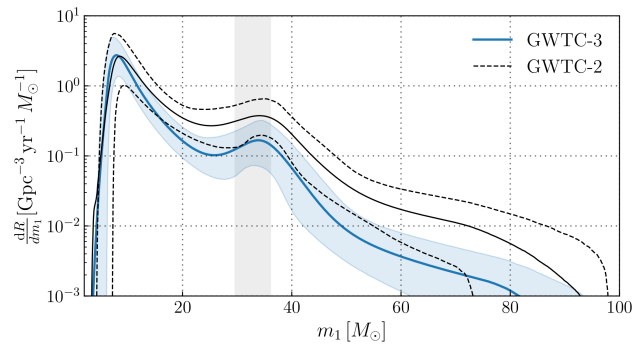


Fig. 7 Binary BH merger rate inferred from GW merger detected as of the publication of the third GW source catalog in LVK collaboration (2023b), as a function of the mass of the most massive BH in the binary (m_1). The curves shown are the results of the “powerlaw+gaussian peak” model fit to the population. Black lines show the results from the second GW catalog (LVK collaboration, 2021a), while blue lines show the most recent results to date (LVK collaboration, 2023a).

7 Known uncertainties

We now discuss the many known uncertainties in the evolution of (P)PISN progenitors. Farmer et al. (2019) performed an extensive survey of stellar evolution uncertainties to assess their impact on the BH masses resulting from (P)PISN. Despite how exotic these explosions may seem, this revealed a surprising robustness of the results within the framework of the evolution of bare He cores. In the following subsections, we focus on the major theoretical uncertainties for (P)PISN identified in Farmer et al. (2019) and subsequent studies (Farmer et al., 2020; Renzo et al., 2020c; Woosley and Heger, 2021; Mehta et al., 2022; Farag et al., 2022; Shen et al., 2023). These add to uncertainties in the general evolution of massive stars discussed elsewhere (e.g., Vink, 2015; Farmer et al., 2016; Renzo et al., 2017; Davis et al., 2019; Josiek et al., 2024).

7.1 Nuclear reaction rates

(P)PISN are caused by a thermonuclear explosion in the star following the collapse caused by pair-production decreasing the radiation pressure support. Therefore, it may not be surprising that uncertainties in the nuclear reaction rates impact (P)PISN. Most of the energy release during the thermonuclear explosion is from $^{16}\text{O} + ^{16}\text{O}$ (when this isotope is present, e.g., Dessart et al. 2013; Marchant et al. 2019), and the biggest uncertainty does not come from the explosive burning itself, but rather from the reactions determining the amount of fuel available to an explosion – in other words, the pre-instability reactions determining the C/O ratio in the core. These are the reaction creating ^{12}C , (3 α , Hoyle, 1954; Farag et al., 2022; Luo et al., 2024) and the reaction destroying it ($^{12}\text{C}(\alpha, \gamma)^{16}\text{O}$, Kunz et al., 2002; deBoer et al., 2017; Shen et al., 2023). The impact of the former on P-PISN was studied in Farag et al. (2022), while the impact of the latter is the focus of Takahashi (2018); Farmer et al. (2019, 2020); Costa et al. (2021); Farag et al. (2022); Mehta et al. (2022); Kawashimo et al. (2023).

Specifically, Takahashi (2018) proposed that a lower $^{12}\text{C}(\alpha, \gamma)^{16}\text{O}$ rate could lead to a sufficiently low ^{16}O mass fraction in the core, pushing the mass range for (P)PISN upward and explaining the lack of observations of these transients. This result was independently confirmed by Farmer et al. (2019) and physically explained in Farmer et al. (2020): with higher C/O ratio a thick convective C burning shell appears in the models, protecting the core from instability by making it effectively evolve as a lower mass CO core. This effect was also seen in the models from Costa et al. (2021) and Woosley and Heger (2021).

However, Mehta et al. (2022) realized that publicly available tables for the rate of $^{12}\text{C}(\alpha, \gamma)^{16}\text{O}$ as a function of temperature were under-resolved: interpolation errors in stellar codes were larger than the 3σ experimental uncertainties (see Figure 7 in Mehta et al. 2022). Their study ammended this and updated the results of Farmer et al. (2020) and made new, more dense, nuclear reaction rates tables available for the community. Figure 8 shows the upper and lower edge of the theoretical PISN BH mass gap from Mehta et al. (2022) as a function of the adopted $^{12}\text{C}(\alpha, \gamma)^{16}\text{O}$ rate.

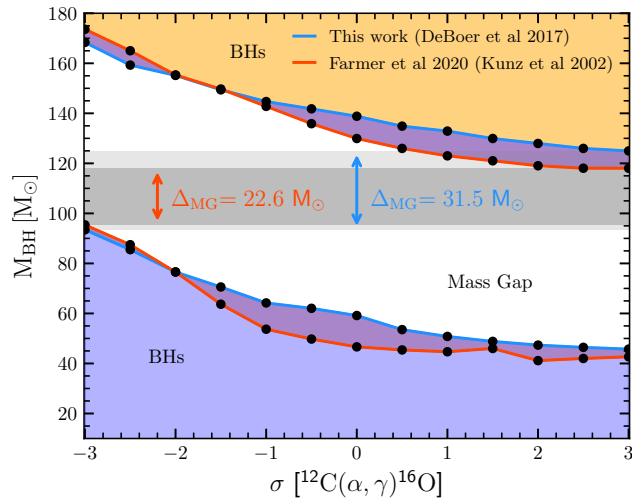


Fig. 8 Lower and upper edge of the PISN BH mass gap as a function of the rate of $^{12}\text{C}(\alpha, \gamma)^{16}\text{O}$ from Mehta et al. (2022) (blue) and Farmer et al. (2019) (red). The caption also indicates the nominal rate adopted (deBoer et al. 2017 in Mehta et al. 2022 and Kunz et al. 2002 in Farmer et al. 2019, respectively), and the x-axis represents the number of standard deviations from the nominal rate. The gray horizontal band represent BH masses that cannot form from single bare He cores, regardless of the $^{12}\text{C}(\alpha, \gamma)^{16}\text{O}$ rate.

Farag et al. (2022) further built upon these results, showing the degeneracy between the assumed nuclear reaction rates and the temporal and spatial resolution required to obtain numerically converged⁴ results. Furthermore, they extented the investigation of nuclear physics uncertainties to the 3α reaction that dominates the production of carbon.

⁴By numerical convergence we mean results not dependent on the choice of spatial and temporal discretization (e.g., Farmer et al., 2016; Farag et al., 2022).

Kawashimo et al. (2023) also showed, albeit with a small 21-isotope nuclear reaction network, that the total amount of radioactive ^{56}Ni produced in PISN full disruptions and the upper boundary of the theorized PISN BH mass gap (see Section 2.4) are also sensitive to the C/O ratio and thus the $^{12}\text{C}(\alpha, \gamma)^{16}\text{O}$ rate, with lower rates producing less radioactive material.

We emphasize that the rates (typically tabulated in stellar evolution codes) are still debated in the nuclear physics community (e.g. Kunz et al., 2002; deBoer et al., 2017; Kibédi et al., 2020; Shen et al., 2023; Luo et al., 2024), and from a stellar perspective, any rate affecting the C/O ratio is expected to impact the (P)PISN process.

7.2 Treatment of convection

Because of its inherent multi-dimensional nature in relation to turbulence, convection is always a major source of uncertainty in stellar evolution calculations. Most models, including of (P)PISN progenitors, rely on mixing length theory (Böhm-Vitense 1958; Jermyn et al. 2022), which is an “effective theory” describing the fully developed convection in steady-state. While this is sufficient for most stellar applications, for (P)PISN progenitors, an additional complication arises: during the dynamical phase (steps 3 and 4 in Figure 2) the evolutionary timescale is shorter than the convective turnover time and the assumption of steady-state breaks down (e.g., Renzo et al., 2020c). A self-consistent spherically-symmetric treatment of the convective acceleration, describing how turbulent energy transport turns on/off in a dynamical and stratified medium is needed to treat the *local* energy transport throughout the structure as the pulse propagates.

If convection efficiently develops during the propagation of a (P)PISN pulse, it can carry energy away until it is radiatively leaked at the surface, weakening the mass loss driven by the pulse, and influence the final BH mass (Renzo et al., 2020c). This is particularly relevant for the lower-mass end of the (P)PISN regime, where different simple treatment of the convective acceleration based on Unno (1967); Arnett (1969); Gough (1977) compared to instantaneous development of convection result in significantly different amount of mass loss. This happens around predicted BH masses of $\sim 35 M_\odot$, a regime now probed directly by both GW detections (LVK collaboration, 2019a; Hendriks et al., 2023) and astrometry (Gaia Collaboration, 2024), which calls for more detailed studies of the development of convection during (P)PISN pulses.

A further uncertainty related to convection is convective boundary mixing (e.g., Umeda et al., 2020; Costa et al., 2021; Vink et al., 2021). This impacts directly the initial mass range and thus predicted rate of (P)PISN: more mixing during the main-sequence leads to more massive He cores and thus more (P)PISN for a given initial mass distribution of stars. Conversely, a smaller amount of mixing will result in smaller cores per a given initial total mass, which can prevent (P)PISN directly, but also influence the stellar structure (Umeda et al., 2020), the C/O ratio in the core (see Section 7.1), the appearance of the star and thus its wind mass loss rate (Vink et al., 2021; Sabhahit et al., 2023). The description of convective boundary mixing remains an open problem and while one-dimensional algorithms for convective boundary mixing informed by three-dimensional simulations exist (e.g., Anders et al., 2022; Johnston et al., 2024), they are not designed for the very high mass regime relevant to (P)PISN.

7.3 Impact of rotation

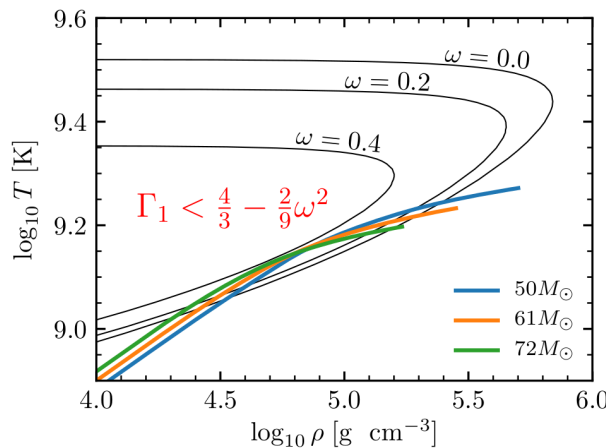


Fig. 9 Instability region on the $T - \rho$ plane modified by the contribution of centrifugal forces to hydrostatic equilibrium from Marchant and Moriya (2020). ω indicates the rotational frequency. Colored tracks are non-rotating ($\omega = 0$) stellar profiles from Marchant et al. (2019) labeled by their total initial He core mass (Marchant et al. 2019 did not include any H-rich envelope in their calculations).

Rotation, much like convection, breaks the spherical symmetry, and for this reason it is a source of uncertainty in one-dimensional stellar calculations. In the context of (P)PISN, one can expect three main effects of rotation:

1. Mixing during the hydrostatic evolution changing the relation between core masses and total initial mass (e.g., Maeder and Meynet, 2000; Chatzopoulos and Wheeler, 2012; Chatzopoulos et al., 2013; Umeda and Nagele, 2024). Similar to increasing main sequence con-

vective boundary mixing, high rotation with efficient associated mixing can increase the expected rate of occurrence of cores sufficiently massive to experience (P)PISN.

2. Centrifugal force changing dynamical equilibrium considerations (see Figure 9). Overall, based on spherically-averaged stellar evolution models, this produces a rather small effect on the final BH masses. The maximum BH mass below the PISN BH mass gap shifts upward by $\sim 4\%$ only when accounting for angular momentum transport (Spruit, 2002) in the star during the pre-pulse hydrostatic evolution (Marchant and Moriya, 2020).
3. Dynamical effect of rotation *during* the pulse generation and propagation (steps 3 and 4 in Figure 2). This has not yet been thoroughly investigated (although see Glatzel et al. 1985).

7.4 Development of asymmetries

Similar to the uncertainties discussed in Section 7.2 and Section 7.3, any other process breaking spherical symmetry that cannot be captured by one-dimensional stellar evolution codes is a source of uncertainty. Asymmetries may develop during the thermonuclear ignition (Renzo et al., 2020b) and during the propagation of a pulse (Chen et al., 2014; Chen et al., 2023).

The former has not yet been thoroughly investigated, but it was suggested as a possibility at the lower mass end of P-PISN in Renzo et al. (2020b) because of the competition between neutrino cooling and energy release by the thermonuclear explosion. In fact, initially in the lowest mass P-PISN models (that is, the ones with the highest core densities at ignition), neutrino cooling dominates over the energy release by the explosion. This means the region of the star where burning is dominating is an off-center shell – a situation reminiscent of other stellar thermonuclear explosions in white dwarfs which could lead to seed asymmetries in the explosion that may be amplified during the pulse propagation.

The other possibility is the development of asymmetries due to Rayleigh-Taylor instabilities during the pulse propagation. Starting with a spherically symmetric explosion, Chen et al. (2014); Chen et al. (2023) showed that these do occur, making multi-dimensional radiation hydrodynamics simulations necessary to obtain detailed light-curves of (P)PISN, but remain overall small in amplitude.

7.5 Binary interactions

Most massive stars are born in binary systems (e.g., Sana et al., 2012; Offner et al., 2023), and the binary fraction does not depend on metallicity (e.g., Moe and Di Stefano, 2017) or maybe increases as metallicity decreases (e.g., Price-Whelan et al. 2020 based on Galactic low mass red giants). Although the binary status of the most massive stars known to date is unclear, these are found in a dense stellar cluster (R136 in the 30 Doradus region, de Koter et al. 1997; Crowther et al. 2010, 2016; Brands et al. 2022) where dynamical processes are likely to pair them into binaries even if they formed as single (e.g., Fujii and Portegies Zwart, 2011). This makes the study of binary interactions among (P)PISN progenitors particularly important and presently lacking, especially in the context of the impact of these explosions on BH masses and GW astronomy.

So far, only calculations based on bare single He cores – assumed to mimic stars stripped of their envelope by a companion long before the (P)PISN onset – have been used to consider the impact of binary interactions (e.g., Marchant et al., 2019; Woosley, 2019; Woosley and Heger, 2021). While this is a useful starting point to discuss, for example, interaction of the expanded post-pulse star with hypothetical companions which could power copious electromagnetic emission (Marchant et al., 2019), it cannot account for the modifications of the core structure due to the timing and amount of mass loss (e.g., Laplace et al., 2021), or address the impact of binary interactions on accretor stars (e.g., Renzo and Götberg, 2021; Miszuda et al., 2021; Renzo et al., 2023; Wagg et al., 2024) or mergers (e.g., Renzo et al., 2020a; Costa et al., 2022; Ballone et al., 2023).

Nevertheless, rapid binary population synthesis calculations use single star models (e.g., from Woosley, 2019) or single bare He core models (e.g., from Marchant et al., 2019; Farmer et al., 2019) to calculate BH masses (Spera et al., 2019; Stevenson et al., 2019; Renzo et al., 2022; Hendriks et al., 2023). Since these models come from numerical simulations distinct from the ones informing BH mass estimates for core-collapse SNe (e.g., Fryer et al., 2012, 2022), this can introduce numerical artifacts resulting in overproduction of BHs at certain masses (e.g., van Son et al., 2022). To avoid this issue, models fitting for the amount of mass lost in detailed stellar evolution simulations of (P)PISN, rather than the resulting BH mass, should be preferred (e.g., Renzo et al., 2022).

Besides modifying the core structure with as-of-yet poorly explored impact on (P)PISN, binary interactions can also alter the BH mass function after the BHs form, through accretion. van Son et al. (2020) showed that this is not expected to produce a detectable effect in the GW mass distribution of BHs: if sufficient accretion can occur, binaries widen too much to become viable GW sources; conversely if accretion is limited by radiation-pressure in the accretion flow (Eddington-limited accretion), the amount of mass accreted is small compared to existing uncertainties in this BH mass regime.

7.6 Fate of the H-rich envelope (if any)

Very massive stars have a few ways to potentially lose their H-rich envelope long before developing a CO core, either through steady stellar winds (e.g., Lucy and Solomon, 1970; Castor et al., 1975; Smith, 2014; Vink, 2015; Renzo et al., 2017; Beasor et al., 2021; Vink et al., 2021; Sabhahit et al., 2023; Decin et al., 2024), binary interactions (e.g., Langer, 2012; Sana et al., 2012; Götberg et al., 2017, 2018), and/or eruptive mass loss (e.g., Smith and Owocki, 2006; Smith et al., 2011b; Smith, 2014; Jiang et al., 2015, 2018; Cheng et al., 2024). Moreover, the main-sequence core-to-envelope mass ratio increases with stellar mass, leading to quasi-homogeneous evolution at finite metallicity (e.g., Yusof et al., 2013; Kozyreva et al., 2017). These arguments are used by many authors to study (P)PISN from bare He cores, since the pair-instability is likely to often start after the H is lost (e.g., Heger and Woosley, 2002; Woosley, 2019), and it is particularly true when focusing on GW sources from isolated binary evolution (e.g., Marchant et al., 2019; Farmer et al., 2019, 2020; Woosley and Heger, 2021;

(Farag et al., 2022), which require final separations of the binary incompatible with an extended H-rich envelope – although in dense stellar environments, BHs may form separately from single star evolution and be dynamically paired afterwards (e.g., Di Carlo et al., 2019; Kremer et al., 2020).

Nevertheless, should a star retain its H-rich envelope until the onset of the pulses, it is then guaranteed to lose it in the first pulse. This can be understood with an energetic argument: typically, extended envelopes have binding energies of $\sim 0.6 - 1 \times 10^{50}$, while pulses release $\gtrsim 10^{50} - 10^{51}$ erg sufficient to unbind the H-layers during the first pulse (e.g., Woosley et al., 2007), as shown by calculations from Woosley et al. (2007); Kasen et al. (2011); Woosley (2017); Leung et al. (2019); Renzo et al. (2020b). In case the entire envelope is not ejected, it will be bloated (e.g., Marchant et al., 2019; Renzo et al., 2020b), lowering its chances to survive the subsequent pulses. Even for cases where a stellar merger adds back a H-rich envelope late in the progenitor evolution, it is unlikely to survive the P-PISN (e.g. Vigna-Gómez et al., 2019).

To determine the lower edge of the PISN BH mass gap (Section 2.4), the remaining issue is what happens to stars just not quite massive enough to encounter the pair-instability with an H-rich envelope. This could occur for single stars at sufficiently low metallicity (preventing efficient wind mass loss, Vink et al. 2021; Sabhahit et al. 2023; Winch et al. 2024), or because of mergers in a dynamical environment (e.g., Di Carlo et al., 2019, 2020a,b; Renzo et al., 2020a; Kremer et al., 2020; Costa et al., 2021, 2022; Ballone et al., 2023) creating a non-standard stellar structure with an under-massive core and oversized envelope. If these envelopes are extended, many mass loss mechanisms are possible at the final collapse (e.g., Quataert et al., 2019; Ivanov and Fernández, 2021; Antoni and Quataert, 2022; Burrows et al., 2023). If instead the envelope is sufficiently compact and manages to avoid eruptive instabilities, and the core is sufficiently small to avoid (P)PISN, it may be possible for it to collapse into a BH swallowing (a large fraction) of the envelope (e.g., Renzo et al., 2020a). One possibility to keep the envelope sufficiently compact, blue, and thus bound is to have small amount of core boundary mixing during the H-burning main-sequence phase (e.g., Umeda et al., 2020), possibly coupled with smaller wind mass-loss rate (e.g., Vink et al., 2021) leading to a small He core-to-envelope mass ratio that favors blue, compact, stellar solutions (e.g., Arnett et al., 1989; Langer et al., 1989). (P)PISN from these progenitor structure are briefly explored in Woosley (2017) and still result in complete envelope removal at the first pulse. PISN from blue supergiants are discussed in Kasen et al. (2011) and Dessart et al. (2013).

7.7 Beyond-standard-model variations

The theory of (P)PISN explosions is rooted in particle physics (cf. Section 2), therefore, it is not surprising that modifications to the standard model may have an impact on the predictions for (P)PISNe. Several beyond-standard-model effects have been included in stellar evolution simulations to test their impact on the minimum CO core mass required for instabilities and on the resulting BH masses. From a stellar evolution point of view, these effects can be studied modifying either the energy generation, hydrostatic equilibrium equations, and/or the equation of state. Beyond-standard-model effects studied so far include:

- Dark matter annihilation (e.g., Ziegler and Freese, 2021; Croon and Sakstein, 2023a). This adds an energy source to the star, whose spatial distribution depends on the assumed mass of the dark matter particle, and may prevent the instability, but only for very high dark matter densities (Croon and Sakstein, 2023a).
- Addition of weakly interacting particles that can escape the star as soon as they are produced (e.g., “hidden” photons – Croon et al. 2020). This adds an energy loss term throughout the evolution of the star, leading to faster nuclear evolution and larger C/O ratios in the core, producing effects similar to lowering the $^{12}\text{C}(\alpha, \gamma)^{16}\text{O}$ rate.
- Addition of more-strongly interacting particles (e.g., axions – Sakstein et al. 2022; Mori et al. 2023). If these couple with photons, this provides an extra channel to lose radiation pressure support on top of Equation 2, exacerbating the pair-production instability.

Whether the proposed modifications are compatible with other existing constraints on beyond-standard-model physics remains to be studied in detail.

8 Conclusions

The study of (P)PISN started almost exactly 60 years ago (Fowler and Hoyle, 1964). Possibly, because of the lack of clear, unambiguous, and uncontroversial observational confirmation, it is characterized by surprising theoretical consensus in terms of the physical evolution of single massive star cores. These are challenged by recent GW detections and many solutions to this apparent discrepancy have already been proposed and are presently hotly debated while further gravitational and electromagnetic detections are collected.

However, we live in a Universe where most massive stars are in multiple systems (e.g., Sana et al., 2012; Offner et al., 2023), a fact seldom included in (P)PISN progenitor modeling, and where the evolution stars we observe with masses well below the threshold for pair-instability still pose theoretical questions. These include their wind mass-loss rates (e.g., Smith, 2014; Vink, 2015; Renzo et al., 2017; Vink et al., 2021; Sabhahit et al., 2023; Winch et al., 2024), their late evolutionary stages (e.g., Farmer et al., 2016; Laplace et al., 2021; Schneider et al., 2024; Renzo et al., 2024) and final collapse (Powell et al., 2021; Rahman et al., 2022). The more massive the star, the more significant theoretical uncertainties (e.g., Agrawal et al., 2022), and the more rare direct observations to improve our models.

Time-domain astronomy allows for probing farther, where progenitors cannot be seen. Despite some initially exciting candidates for PISNe from modern surveys, it remains unclear that we have actually observed one. Very recently, Schulze et al. (2024) put forward SN2018ibb as the best candidate to date. For P-PISNe, there appears to be few very strong case of a P-PISN (e.g., SN 2010mb, Ben-Ami et al. 2014, iPTF16eh, Lunnan et al. 2018, and SN 1961V, Woosley and Smith 2022), accompanied by a few other candidates (SN 2006jc; SN 2006gy; and by extension, some other SLSNe IIn if they do not show broad H lines). Transients caused by the pair instability are

therefore likely to be quite rare. Whether this is consistent with expected rates for their initial mass ranges remains somewhat uncertain, and may depend on the star formation and evolution models. It may also depend strongly on our ability to correctly diagnose a pair-instability event when we see it. As noted above, true PISNe should be relatively straightforward to identify, whereas the diverse outcomes of P-PISNe might likely be misclassified and may still be lurking among samples of observed transients.

8.1 Future prospects

The opportunities to shed light on the fate of the most massive stars are plentiful. JWST is currently operating, so perhaps the lack of unambiguous direct electromagnetic detections will change soon (Hummel et al., 2012; Whalen et al., 2013; Regos et al., 2020). Future missions such as ROMAN (Moriya et al., 2023) and Euclid (Moriya et al., 2022; Tanikawa et al., 2022) may also find PISN and P-PISN transients. Ground based surveys such as Rubin/LSST will also contribute, especially in the search for slowly evolving transients such as those predicted for PISNe.

Moreover, GW detection of merging binary BH will continue. The LIGO-Virgo-KAGRA observing runs O4 (ongoing at the time of writing) and O5 (ending in 2029) will provide better statistics to understand the population of *merging* binary BHs (a very small fraction of the total, but nevertheless informative). Farther in the future, 3rd generation ground-based detectors promise to detect every binary BH merger up to redshifts beyond the predicted formation of the first stars – possibly revealing a fuller picture.

Finally, the wide-spread availability of stellar evolution codes capable of alternating between hydrostatic and dynamical phases of evolution during pulses has allowed for the first time to start exploring the theoretical and input physics uncertainties. The role of pre-pulse binary interactions remain so far unexplored, but are likely relevant for the formation of GW sources and observational transients, and some relevant physics (mixing, nuclear reaction rates, opacities) is still being updated, making this field ripe for advances.

Acknowledgments

MR is grateful to D. Hendriks, S. Justham, L. van Son, R. Farmer, and S. E. de Mink, for many illuminating discussions on the (astro)physics of these explosions over the years, to P. Marchant and especially R. Farmer for invaluable help in making simulations of (P)PISN possible with a community-driven and open-source code (MESA), and to D. Croon for feedback on beyond-standard-model modifications to (P)PISN. We also emphasize the pioneering role of S. Woosley in developing the theory of (P)PISN which has been an inspiration throughout the years.

See Also: Marchant et al. (2019) provide at <https://zenodo.org/records/3786599> movies for the evolution of several quantities during the P-PISN of massive He cores. We also refer readers to Lin et al. (2023); Kuncarayakti et al. (2023); Aamer et al. (2024); Sharma et al. (2024) for other transients discussed in the context of (P)PISN not covered above.

References

Aamer A, Nicholl M, Jerkstrand A, Gomez S, Oates SR, Smartt SJ, Srivastav S, Leloudas G, Anderson JP, Berger E, de Boer T, Chambers K, Chen TW, Galbany L, Gao H, Gompertz BP, González-Baños M, Gromadzki M, Gutiérrez CP, Inserra C, Lowe TB, Magnier EA, Mazzali PA, Moore T, Müller-Bravo TE, Pursiainen M, Rest A, Schulze S, Smith KW, Terwel JH, Wainscoat R and Young DR (2024), Feb. A precursor plateau and pre-maximum [O II] emission in the superluminous SN2019szu: a pulsational pair-instability candidate. *MNRAS* 527 (4): 11970–11995. doi:10.1093/mnras/stad3776. 2307. 02487.

Agrawal P, Szécsi D, Stevenson S, Eldridge JJ and Hurley J (2022), Jun. Explaining the differences in massive star models from various simulations. *MNRAS* 512 (4): 5717–5725. doi:10.1093/mnras/stac930. 2112. 02800.

Anders EH, Jermyn AS, Lecoanet D and Brown BP (2022), Feb. Stellar Convective Penetration: Parameterized Theory and Dynamical Simulations. *ApJ* 926 (2), 169. doi:10.3847/1538-4357/ac408d. 2110. 11356.

Andrews JE and Smith N (2018), Jun. Strong late-time circumstellar interaction in the peculiar supernova iPTF14hls. *MNRAS* 477 (1): 74–79. doi:10.1093/mnras/sty584. 1712. 00514.

Antoni A and Quataert E (2022), Mar. Numerical simulations of the random angular momentum in convection: Implications for supergiant collapse to form black holes. *MNRAS* 511 (1): 176–197. doi:10.1093/mnras/stab3776. 2107. 09068.

Aoki W, Tominaga N, Beers TC, Honda S and Lee YS (2014), Aug. A chemical signature of first-generation very massive stars. *Science* 345 (6199): 912–915. doi:10.1126/science.1252633.

Arcavi I, Howell DA, Kasen D, Bildsten L, Hosseinzadeh G, McCully C, Wong ZC, Katz SR, Gal-Yam A, Sollerman J, Taddia F, Leloudas G, Fremling C, Nugent PE, Horesh A, Mooley K, Rumsey C, Cenko SB, Graham ML, Perley DA, Nakar E, Shaviv NJ, Bromberg O, Shen KJ, Ofek EO, Cao Y, Wang X, Huang F, Rui L, Zhang T, Li W, Li Z, Zhang J, Valenti S, Guevel D, Shappee B, Kochanek CS, Holoiien TWS, Filippenko AV, Fender R, Nyholm A, Yaron O, Kasliwal MM, Sullivan M, Blagorodnova N, Walters RS, Lunnan R, Khazov D, Andreoni I, Laher RR, Konidaris N, Woziak P and Bue B (2017), Nov. Energetic eruptions leading to a peculiar hydrogen-rich explosion of a massive star. *Nature* 551 (7679): 210–213. doi:10.1038/nature24030. 1711. 02671.

Arnett WD (1969), Oct. A Possible Model of Supernovae: Detonation of ^{12}C . *Astrophys. Space Sci.* 5: 180–212. doi:10.1007/BF00650291.

Arnett WD, Bahcall JN, Kirshner RP and Woosley SE (1989), Jan. Supernova 1987A. *ARAA* 27: 629–700. doi:10.1146/annurev.aa.27.090189. 003213.

Ballone A, Costa G, Mapelli M, MacLeod M, Tornamenti S and Pacheco-Arias JM (2023), Mar. Formation of black holes in the pair-instability mass gap: hydrodynamical simulations of a head-on massive star collision. *MNRAS* 519 (4): 5191–5201. doi:10.1093/mnras/stac3752. 2204. 03493.

Barkat Z, Rakavy G and Sack N (1967), Mar. Dynamics of Supernova Explosion Resulting from Pair Formation. *Physical Review Letters* 18: 379–381. doi:10.1103/PhysRevLett.18.379.

Beasor ER, Davies B and Smith N (2021), Nov. The Impact of Realistic Red Supergiant Mass Loss on Stellar Evolution. *ApJ* 922 (1), 55. doi:10.3847/1538-4357/ac2574. 2109.03239.

Ben-Ami S, Gal-Yam A, Mazzali PA, Gnat O, Modjaz M, Rabinak I, Sullivan M, Bildsten L, Poznanski D, Yaron O, Arcavi I, Bloom JS, Horesh A, Kasliwal MM, Kulkarni SR, Nugent PE, Ofek EO, Perley D, Quimby R and Xu D (2014), Apr. SN 2010mb: Direct Evidence for a Supernova Interacting with a Large Amount of Hydrogen-free Circumstellar Material. *ApJ* 785 (1), 37. doi:10.1088/0004-637X/785/1/37. 1309.6496.

Bertola F (1963), Jan. Spectrum and light curve of the variable object near NGC 1058. *Contributi dell'Osservatorio Astrofisica dell'Università di Padova in Asiago* 142: 3.

Böhm-Vitense E (1958), Jan. Über die Wasserstoffkonvektionszone in Sternen verschiedener Effektivtemperaturen und Leuchtkräfte. Mit 5 Textabbildungen. *Zeit. Astr.* 46: 108.

Bond JR, Arnett WD and Carr BJ (1984), May. The evolution and fate of Very Massive Objects. *ApJ* 280: 825–847. doi:10.1086/162057.

Branch D and Greenstein JL (1971), Jul. The 1961 Supernova in NGC 1058. *ApJ* 167: 89. doi:10.1086/151007.

Brands SA, de Koter A, Bestenlehner JM, Crowther PA, Sundqvist JO, Puls J, Caballero-Nieves SM, Abdul-Masih M, Driessen FA, García M, Geen S, Gräfener G, Hawcroft C, Kaper L, Keszthelyi Z, Langer N, Sana H, Schneider FRN, Shenar T and Vink JS (2022), Jul. The R136 star cluster dissected with Hubble Space Telescope/STIS. III. The most massive stars and their clumped winds. *A&A* 663, A36. doi:10.1051/0004-6361/202142742. 2202.11080.

Breit G and Wheeler JA (1934), Dec. Collision of Two Light Quanta. *Physical Review* 46 (12): 1087–1091. doi:10.1103/PhysRev.46.1087.

Briel MM, Stevance HF and Eldridge JJ (2023), Apr. Understanding the high-mass binary black hole population from stable mass transfer and super-Eddington accretion in BPASS. *MNRAS* 520 (4): 5724–5745. doi:10.1093/mnras/stad399. 2206.13842.

Burrows A and Vartanyan D (2021), Jan. Core-collapse supernova explosion theory. *Nature* 589 (7840): 29–39. doi:10.1038/s41586-020-03059-w. 2009.14157.

Burrows A, Vartanyan D and Wang T (2023), Nov. Black Hole Formation Accompanied by the Supernova Explosion of a 40 M_⊙ Progenitor Star. *ApJ* 957 (2), 68. doi:10.3847/1538-4357/acfc1c. 2308.05798.

Callister TA and Farr WM (2024), Apr. Parameter-Free Tour of the Binary Black Hole Population. *Physical Review X* 14 (2), 021005. doi:10.1103/PhysRevX.14.021005. 2302.07289.

Castor JI, Abbott DC and Klein RI (1975), Jan. Radiation-driven winds in Of stars. *ApJ* 195: 157–174. doi:10.1086/153315.

Chatzopoulos E and Wheeler JC (2012), Mar. Effects of Rotation on the Minimum Mass of Primordial Progenitors of Pair-instability Supernovae. *ApJ* 748, 42. doi:10.1088/0004-637X/748/1/42. 1201.1328.

Chatzopoulos E, Wheeler JC and Couch SM (2013), Oct. Multi-dimensional Simulations of Rotating Pair-instability Supernovae. *ApJ* 776, 129. doi:10.1088/0004-637X/776/2/129. 1308.4660.

Chen KJ, Woosley S, Heger A, Almgren A and Whalen DJ (2014). Two-dimensional simulations of pulsational pair-instability supernovae. *The Astrophysical Journal* 792 (1): 28. <http://stacks.iop.org/0004-637X/792/1-1/a=28>.

Chen KJ, Whalen DJ, Woosley SE and Zhang W (2023), Sep. Multidimensional Radiation Hydrodynamics Simulations of Pulsational Pair-instability Supernovae. *ApJ* 955 (1), 39. doi:10.3847/1538-4357/ace968.

Cheng SJ, Goldberg JA, Cantiello M, Bauer EB, Renzo M and Conroy C (2024), May. A Model for Eruptive Mass Loss in Massive Stars. *arXiv e-prints*, arXiv:2405.12274doi:10.48550/arXiv.2405.12274. 2405.12274.

Clark DH and Stephenson FR (1977). The historical supernovae, Oxford.

Costa G, Bressan A, Mapelli M, Marigo P, Iorio G and Spera M (2021), Mar. Formation of GW190521 from stellar evolution: the impact of the hydrogen-rich envelope, dredge-up, and ¹²C(α, γ)¹⁶O rate on the pair-instability black hole mass gap. *MNRAS* 501 (3): 4514–4533. doi:10.1093/mnras/staa3916. 2010.02242.

Costa G, Ballone A, Mapelli M and Bressan A (2022), Oct. Formation of black holes in the pair-instability mass gap: Evolution of a post-collision star. *MNRAS* 516 (1): 1072–1080. doi:10.1093/mnras/stac2222. 2204.03492.

Costa G, Chruścińska M, Klencki J, Broekgaarden FS, Rodriguez CL, Joseph TD and Saracino S (2023), Nov. Stellar Black Holes and Compact Stellar Remnants. *arXiv e-prints*, arXiv:2311.15778doi:10.48550/arXiv.2311.15778. 2311.15778.

Croon D and Sakstein J (2023a), Oct. Dark Matter Annihilation and Pair-Instability Supernovae. *arXiv e-prints*, arXiv:2310.20044doi:10.48550/arXiv.2310.20044. 2310.20044.

Croon D and Sakstein J (2023b), Dec. Prediction of Multiple Features in the Black Hole Mass Function due to Pulsational Pair-Instability Supernovae. *arXiv e-prints*, arXiv:2312.13459doi:10.48550/arXiv.2312.13459. 2312.13459.

Croon D, McDermott SD and Sakstein J (2020), Jul. Missing in Action: New Physics and the Black Hole Mass Gap. *arXiv e-prints*, arXiv:2007.07889doi:10.48550/arXiv.2007.07889. 2007.07889.

Crowther PA, Schnurr O, Hirschi R, Yusof N, Parker RJ, Goodwin SP and Kassim HA (2010), Oct. The R136 star cluster hosts several stars whose individual masses greatly exceed the accepted 150M_{solar} stellar mass limit. *MNRAS* 408: 731–751. doi:10.1111/j.1365-2966.2010.17167.x. 1007.3284.

Crowther PA, Caballero-Nieves SM, Bostroem KA, Maíz Apellániz J, Schneider FRN, Walborn NR, Angus CR, Brott I, Bonanos A, de Koter A, de Mink SE, Evans CJ, Gräfener G, Herrero A, Howarth ID, Langer N, Lennon DJ, Puls J, Sana H and Vink JS (2016), May. The R136 star cluster dissected with Hubble Space Telescope/STIS. I. Far-ultraviolet spectroscopic census and the origin of He II λ1640 in young star clusters. *MNRAS* 458: 624–659. doi:10.1093/mnras/stw273. 1603.04994.

Davis A, Jones S and Herwig F (2019), Apr. Convective boundary mixing in a post-He core burning massive star model. *MNRAS* 484 (3): 3921–3934. doi:10.1093/mnras/sty3415. 1712.00114.

de Koter A, Heap SR and Hubeny I (1997), Mar. On the Evolutionary Phase and Mass Loss of the Wolf-Rayet-like Stars in R136a. *ApJ* 477: 792. doi:10.1086/303736.

deBoer RJ, Görres J, Wiescher M, Azuma RE, Best A, Brune CR, Fields CE, Jones S, Pignatari M, Sayre D, Smith K, Timmes FX and Uberseder E (2017), Jul. The ¹²C(α, γ)¹⁶O reaction and its implications for stellar helium burning. *Reviews of Modern Physics* 89 (3), 035007. doi:10.1103/RevModPhys.89.035007. 1709.03144.

Decin L, Richards AMS, Merchant P and Sana H (2024), Jan. ALMA detection of CO rotational line emission in red supergiant stars of the massive young star cluster RSGC1. Determination of a new mass-loss rate prescription for red supergiants. *A&A* 681, A17. doi:10.1051/0004-6361/202244635. 2303.09385.

Dessart L (2024), May. Interacting supernovae. *arXiv e-prints*, arXiv:2405.04259doi:10.48550/arXiv.2405.04259. 2405.04259.

Dessart L, Waldman R, Livne E, Hillier DJ and Blondin S (2013), Feb. Radiative properties of pair-instability supernova explosions. *MNRAS* 428 (4): 3227–3251. doi:10.1093/mnras/sts269. 1210.6163.

Di Carlo UN, Giacobbo N, Mapelli M, Pasquato M, Spera M, Wang L and Haardt F (2019), Aug. Merging black holes in young star clusters. *MNRAS* 487 (2): 2947–2960. doi:10.1093/mnras/stz1453. 1901.00863.

Di Carlo UN, Mapelli M, Bouffanais Y, Giacobbo N, Santoliquido F, Bressan Ar, Spera M and Haardt F (2020a), Jul. Binary black holes in the pair instability mass gap. *MNRAS* 497 (1): 1043–1049. doi:10.1093/mnras/staa1997. 1911.01434.

Di Carlo UN, Mapelli M, Giacobbo N, Spera M, Bouffanais Y, Rastello S, Santoliquido F, Pasquato M, Ballone Ar, Trani AA, Torniamenti S and Haardt F (2020b), Aug. Binary black holes in young star clusters: the impact of metallicity. *MNRAS* 498 (1): 495–506. doi:10.1093/mnras/staa2286. 2004.09525.

Doherty CL, Gil-Pons P, Siess L, Lattanzio JC and Lau HHB (2015), Jan. Super- and massive AGB stars - IV. Final fates - initial-to-final mass relation. *MNRAS* 446 (3): 2599–2612. doi:10.1093/mnras/stu2180. 1410.5431.

Edelman B, Doctor Z and Farr B (2021), Jun. Poking Holes: Looking for Gaps in LIGO/Virgo's Black Hole Population. *ApJL* 913 (2), L23. doi:10.3847/2041-8213/abfdb3. 2104.07783.

Eggenberger P, Meynet G, Maeder A, Hirschi R, Charbonnel C, Talon S and Ekström S (2008), Aug. The Geneva stellar evolution code. *Astrophys. Space Sci.* 316 (1-4): 43–54. doi:10.1007/s10509-007-9511-y.

Farag E, Timmes FX, Taylor M, Patton KM and Farmer R (2020), Apr. On Stellar Evolution in a Neutrino Hertzsprung-Russell Diagram. *ApJ* 893 (2), 133. doi:10.3847/1538-4357/ab7f2c. 2003.05844.

Farag E, Renzo M, Farmer R, Chidester MT and Timmes FX (2022), Oct. Resolving the Peak of the Black Hole Mass Spectrum. *ApJ* 937 (2), 112. doi:10.3847/1538-4357/ac8b83. 2208.09624.

Farmer R, Fields CE, Petermann I, Dessart L, Cantiello M, Paxton B and Timmes FX (2016), Dec. On Variations Of Pre-supernova Model Properties. *ApJS* 227, 22. doi:10.3847/1538-4365/227/2/22. 1611.01207.

Farmer R, Renzo M, de Mink SE, Marchant P and Justham S (2019), Dec. Mind the Gap: The Location of the Lower Edge of the Pair-instability Supernova Black Hole Mass Gap. *ApJ* 887 (1), 53. doi:10.3847/1538-4357/ab518b. 1910.12874.

Farmer R, Renzo M, de Mink SE, Fishbach M and Justham S (2020), Oct. Constraints from Gravitational-wave Detections of Binary Black Hole Mergers on the $^{12}\text{C}(\alpha, \gamma)^{16}\text{O}$ Rate. *ApJL* 902 (2), L36. doi:10.3847/2041-8213/abbadd. 2006.06678.

Farr WM, Sravan N, Cantrell A, Kreidberg L, Bailyn CD, Mandel I and Kalogera V (2011), Nov. The Mass Distribution of Stellar-mass Black Holes. *ApJ* 741, 103. doi:10.1088/0004-637X/741/2/103. 1011.1459.

Farr WM, Fishbach M, Ye J and Holz DE (2019), Oct. A Future Percent-level Measurement of the Hubble Expansion at Redshift 0.8 with Advanced LIGO. *ApJL* 883 (2), L42. doi:10.3847/2041-8213/ab4284. 1908.09084.

Filippenko AV, Barth AJ, Bower GC, Ho LC, Stringfellow GS, Goodrich RW and Porter AC (1995), Nov. Was Fritz Zwicky's "Type V" SN 1961V a Genuino Supernova? *AJ* 110: 2261. doi:10.1086/117687.

Fishbach M and Holz DE (2020), Dec. Minding the Gap: GW190521 as a Straddling Binary. *ApJL* 904 (2), L26. doi:10.3847/2041-8213/abc827. 2009.05472.

Fowler WA and Hoyle F (1964), Dec. Neutrino Processes and Pair Formation in Massive Stars and Supernovae. *ApJS* 9: 201. doi:10.1086/190103.

Fraley GS (1968), Aug. Supernovae Explosions Induced by Pair-Production Instability. *Astrophys. Space Sci.* 2: 96–114. doi:10.1007/BF00651498.

Fraser M, Inserra C, Jerkstrand A, Kotak R, Pignata G, Benetti S, Botticella MT, Bufano F, Childress M, Mattila S, Pastorello A, Smartt SJ, Turatto M, Yuan F, Anderson JP, Bayliss DDR, Bauer FE, Chen TW, Förster Burón F, Gal-Yam A, Haislip JB, Knapic C, Le Guillou L, Marchi S, Mazzali P, Molinaro M, Moore JP, Reichart D, Smareglia R, Smith KW, Sternberg A, Sullivan M, Takáts K, Tucker BE, Valenti S, Yaron O, Young DR and Zhou G (2013), Aug. SN 2009ip à la PESSTO: no evidence for core collapse yet. *MNRAS* 433 (2): 1312–1337. doi:10.1093/mnras/stt813. 1303.3453.

Fryer CL, Woosley SE and Heger A (2001), Mar. Pair-Instability Supernovae, Gravity Waves, and Gamma-Ray Transients. *ApJ* 550: 372–382. doi:10.1086/319719. astro-ph/0007176.

Fryer CL, Belczynski K, Wiktorowicz G, Dominik M, Kalogera V and Holz DE (2012), Apr. Compact Remnant Mass Function: Dependence on the Explosion Mechanism and Metallicity. *ApJ* 749, 91. doi:10.1088/0004-637X/749/1/91. 1110.1726.

Fryer CL, Olejak A and Belczynski K (2022), Jun. The Effect of Supernova Convection On Neutron Star and Black Hole Masses. *ApJ* 931 (2), 94. doi:10.3847/1538-4357/ac6ac9. 2204.13025.

Fryxell B, Olson K, Ricker P, Timmes FX, Zingale M, Lamb DQ, MacNeice P, Rosner R, Truran JW and Tufo H (2000), Nov. FLASH: An Adaptive Mesh Hydrodynamics Code for Modeling Astrophysical Thermonuclear Flashes. *ApJS* 131 (1): 273–334. doi:10.1086/317361.

Fujii MS and Portegies Zwart S (2011), Dec. The Origin of OB Runaway Stars. *Science* 334: 1380. doi:10.1126/science.1211927. 1111.3644.

Gaia Collaboration (2024), Apr. Discovery of a dormant 33 solar-mass black hole in pre-release Gaia astrometry. *arXiv e-prints*, arXiv:2404.10486 doi:10.48550/arXiv.2404.10486. 2404.10486.

Gal-Yam A, Mazzali P, Ofek EO, Nugent PE, Kulkarni SR, Kasliwal MM, Quimby RM, Filippenko AV, Cenko SB, Chornock R, Waldman R, Kasen D, Sullivan M, Beshore EC, Drake AJ, Thomas RC, Bloom JS, Poznanski D, Miller AA, Foley RJ, Silverman JM, Arcavi I, Ellis RS and Deng J (2009), Dec. Supernova 2007bi as a pair-instability explosion. *Nature* 462 (7273): 624–627. doi:10.1038/nature08579. 1001.1156.

Georgy C, Meynet G, Ekström S, Wade GA, Petit V, Keszthelyi Z and Hirschi R (2017), Mar. Possible pair-instability supernovae at solar metallicity from magnetic stellar progenitors. *A&A* 599, L5. doi:10.1051/0004-6361/201730401. 1702.02340.

Glatzel W, Fricke KJ and El Eid MF (1985), Aug. The fate of rotating pair-unstable carbon-oxygen cores. *A&A* 149: 413–422.

Golomb J, Iyi M and Farr W (2023), Dec. Physical Models for the Astrophysical Population of Black Holes: Application to the Bump in the Mass Distribution of Gravitational Wave Sources. *arXiv e-prints*, arXiv:2312.03973 doi:10.48550/arXiv.2312.03973. 2312.03973.

Gomez S, Berger E, Nicholl M, Blanchard PK, Villar VA, Patton L, Chornock R, Leja J, Hosseinzadeh G and Cowperthwaite PS (2019), Aug. SN 2016iet: The Pulsational or Pair Instability Explosion of a Low-metallicity Massive CO Core Embedded in a Dense Hydrogen-poor Circumstellar Medium. *ApJ* 881 (2), 87. doi:10.3847/1538-4357/ab2f92. 1904.07259.

Goodrich RW, Stringfellow GS, Penrod GD and Filippenko AV (1989), Jul. SN 1961V: an Extragalactic Eta Carinae Analog? *ApJ* 342: 908. doi:10.1086/167646.

Götzberg Y, de Mink SE and Groh JH (2017), Jan. Ionizing spectra of stars that lose their envelope through interaction with a binary companion: role of metallicity. *ArXiv e-prints* 1701.07439.

Götzberg Y, de Mink SE, Groh JH, Kupfer T, Crowther PA, Zapartas E and Renzo M (2018), Jul. Spectral models for binary products: Unifying subdwarfs and Wolf-Rayet stars as a sequence of stripped-envelope stars. *A&A* 615, A78. doi:10.1051/0004-6361/201732274. 1802.03018.

Gough DO (1977), May. Mixing-length theory for pulsating stars. *ApJ* 214: 196–213. doi:10.1086/155244.

Greene JE, Strader J and Ho LC (2020), Aug. Intermediate-Mass Black Holes. *ARAA* 58: 257–312. doi:10.1146/annurev-astro-032620-021835. 1911.09678.

Gronow S, Côté B, Lach F, Seitzenzahl IR, Collins CE, Sim SA and Röpke FK (2021), Dec. Metallicity-dependent nucleosynthetic yields of Type Ia supernovae originating from double detonations of sub- M_{Ch} white dwarfs. *A&A* 656, A94. doi:10.1051/0004-6361/202140881. 2103.14050.

Heger A and Woosley SE (2002), Mar. The Nucleosynthetic Signature of Population III. *ApJ* 567: 532–543. doi:10.1086/338487. astro-ph/0107037.

Heger A, Fryer CL, Woosley SE, Langer N and Hartmann DH (2003), Jul. How Massive Single Stars End Their Life. *ApJ* 591: 288–300. doi:10.1086/375341. astro-ph/0212469.

Hendriks DD, van Son LAC, Renzo M, Izzard RG and Farmer R (2023), Dec. Pulsational pair-instability supernovae in gravitational-wave and electromagnetic transients. *MNRAS* 526 (3): 4130–4147. doi:10.1093/mnras/stad2857. 2309.09339.

Hoyle F (1954), Sep. On Nuclear Reactions Occuring in Very Hot STARS.I. the Synthesis of Elements from Carbon to Nickel. *ApJS* 1: 121. doi:10.1086/190005.

Hummel JA, Pawlik AH, Milosavljević M and Bromm V (2012), Aug. The Source Density and Observability of Pair-instability Supernovae from the First Stars. *ApJ* 755 (1), 72. doi:10.1088/0004-637X/755/1/72. 1112.5207.

Humphreys RM, Davidson K and Smith N (1999), Sep. η Carinae's Second Eruption and the Light Curves of the η Carinae Variables. *PASP* 111 (763): 1124–1131. doi:10.1086/316420.

Ivanov M and Fernández R (2021), Apr. Mass Ejection in Failed Supernovae: Equation of State and Neutrino Loss Dependence. *ApJ* 911 (1), 6. doi:10.3847/1538-4357/abe59e. 2101.02712.

Janka HT (2012), Nov. Explosion Mechanisms of Core-Collapse Supernovae. *Annual Review of Nuclear and Particle Science* 62 (1): 407–451. doi:10.1146/annurev-nucl-102711-094901. 1206.2503.

Jermyn AS, Anders EH, Lecoanet D and Cantiello M (2022), Sep. An Atlas of Convection in Main-sequence Stars. *ApJS* 262 (1), 19. doi:10.3847/1538-4365/ac7ee. 2206.00011.

Jermyn AS, Bauer EB, Schwab J, Farmer R, Ball WH, Bellinger EP, Dotter A, Joyce M, Marchant P, Mombarg JSG, Wolf WM, Sunny Wong TL, Cinquegrana GC, Farrell E, Smolec R, Thoul A, Cantiello M, Herwig F, Toloza O, Bildsten L, Townsend RHD and Timmes FX (2023), Mar. Modules for Experiments in Stellar Astrophysics (MESA): Time-dependent Convection, Energy Conservation, Automatic Differentiation, and Infrastructure. *ApJS* 265 (1), 15. doi:10.3847/1538-4365/acae8d. 2208.03651.

Jiang YF, Cantiello M, Bildsten L, Quataert E and Blaes O (2015), Nov. Local Radiation Hydrodynamic Simulations of Massive Star Envelopes at the Iron Opacity Peak. *ApJ* 813 (1), 74. doi:10.1088/0004-637X/813/1/74. 1509.05417.

Jiang YF, Cantiello M, Bildsten L, Quataert E, Blaes O and Stone J (2018), Sep. Outbursts of luminous blue variable stars from variations in the helium opacity. *Nature* 561 (7724): 498–501. doi:10.1038/s41586-018-0525-0. 1809.10187.

Johnston C, Michelsen M, Anders EH, Renzo M, Cantiello M, Marchant P, Goldberg JA, Townsend RHD, Sabhahit G and Jermyn AS (2024), Apr. Modelling Time-dependent Convective Penetration in 1D Stellar Evolution. *ApJ* 964 (2), 170. doi:10.3847/1538-4357/ad2343. 2312.08315.

Josiek J, Ekström S and Sander AAC (2024), Apr. Impact of main-sequence mass loss on the appearance, structure and evolution of Wolf-Rayet stars. *arXiv e-prints*, arXiv:2404.14488doi:10.48550/arXiv.2404.14488. 2404.14488.

Kasen D and Bildsten L (2010), Jul. Supernova Light Curves Powered by Young Magnetars. *ApJ* 717 (1): 245–249. doi:10.1088/0004-637X/717/1/245. 0911.0680.

Kasen D, Woosley SE and Heger A (2011), Jun. Pair Instability Supernovae: Light Curves, Spectra, and Shock Breakout. *ApJ* 734 (2), 102. doi:10.1088/0004-637X/734/2/102. 1101.3336.

Kawashimo H, Sawada R, Suwa Y, Moriya TJ, Tanikawa A and Tominaga N (2023), Jun. Impacts of the $^{12}\text{C}(\alpha, \gamma)^{16}\text{O}$ reaction rate on ^{56}Ni nucleosynthesis in pair-instability supernovae. *arXiv e-prints*, arXiv:2306.01682doi:10.48550/arXiv.2306.01682. 2306.01682.

Keszthelyi Z, Meynet G, Georgy C, Wade GA, Petit V and David-Uraz A (2019), Jun. The effects of surface fossil magnetic fields on massive star evolution: I. Magnetic field evolution, mass-loss quenching, and magnetic braking. *MNRAS* 485 (4): 5843–5860. doi:10.1093/mnras/stz772. 1902.09333.

Kibédi T, Alshahrani B, Stuchbery AE, Larsen AC, Görgen A, Siem S, Guttormsen M, Giacoppo F, Morales AI, Sahin E, Tveten GM, Garrote FLB, Campo LC, Eriksen TK, Klintefjord M, Maharramova S, Nyhus HT, Tornyi TG, Renstrøm T and Paulsen W (2020), Oct. Radiative width of the hoyle state from γ -ray spectroscopy. *Phys. Rev. Lett.* 125: 182701. doi:10.1103/PhysRevLett.125.182701. <https://link.aps.org/doi/10.1103/PhysRevLett.125.182701>.

Kippenhahn R, Weigert A and Weiss A (2013), *Stellar Structure and Evolution*, Springer-Verlag. doi:10.1007/978-3-642-30304-3.

Kozyreva A, Gilmer M, Hirschi R, Fröhlich C, Blinnikov S, Wollaeger RT, Noebauer UM, van Rossum DR, Heger A, Even WP, Waldman R, Tolstov A, Chatzopoulos E and Sorokina E (2017), Jan. Fast evolving pair-instability supernova models: evolution, explosion, light curves. *MNRAS* 464 (3): 2854–2865. doi:10.1093/mnras/stw2562. 1610.01086.

Kremer K, Spera M, Becker D, Chatterjee S, Di Carlo UN, Fragione G, Rodriguez CL, Ye CS and Rasio FA (2020), Jun. Populating the upper black hole mass gap through stellar collisions in young star clusters. *arXiv e-prints*, arXiv:2006.107712006.10771.

Kroupa P (2001), Apr. On the variation of the initial mass function. *MNRAS* 322: 231–246. doi:10.1046/j.1365-8711.2001.04022.x. astro-ph/0009005.

Kuncarayakti H, Sollerman J, Izzo L, Maeda K, Yang S, Schulze S, Angus CR, Aubert M, Auchettl K, Della Valle M, Dessart L, Hinds K, Kankare E, Kawabata M, Lundqvist P, Nakaoka T, Perley D, Raimundo SI, Strotjohann NL, Taguchi K, Cai YZ, Charalampopoulos P, Fang Q, Fraser M, Gutiérrez CP, Imazawa R, Kangas T, Kawabata KS, Kotak R, Kravtsov T, Matilainen K, Mattila S, Moran S, Murata I, Salmaso I, Anderson JP, Ashall C, Bellm EC, Benetti S, Chambers KC, Chen TW, Coughlin M, De Colle F, Fremling C, Galbany L, Gal-Yam A, Gromadzki M, Groom SL, Hajela A, Inserra C, Kasliwal MM, Mahabal AA, Martin-Carrillo A, Moore T, Müller-Bravo TE, Nicholl M, Ragosta F, Riddle RL, Sharma Y, Srivastav S, Stritzinger MD, Wold A and Young DR (2023), Oct. The broad-lined Type-Ic supernova SN 2022xxf and its extraordinary two-humped light curves. I. Signatures of H/He-free interaction in the first four months. *A&A* 678, A209. doi:10.1051/0004-6361/202346526. 2303.16925.

Kunz R, Fey M, Jaeger M, Mayer A, Hammer JW, Staudt G, Harissopoulos S and Paradellis T (2002), Mar. Astrophysical Reaction Rate of $^{12}\text{C}(\alpha, \gamma)^{16}\text{O}$. *ApJ* 567 (1): 643–650. doi:10.1086/338384.

Kuroda T, Kotake K, Takiwaki T and Thielemann FK (2018), Jun. A full general relativistic neutrino radiation-hydrodynamics simulation of a collapsing very massive star and the formation of a black hole. *MNRAS* 477: L80–L84. doi:10.1093/mnrasl/sly059. 1801.01293.

Langer N (2012), Sep. Presupernova Evolution of Massive Single and Binary Stars. *ARA&A* 50: 107–164. doi:10.1146/annurev-astro-081811-125534. 1206.5443.

Langer N, El Eid MF and Baraffe I (1989), Oct. Blue supergiant supernova progenitors. *A&A* 224: L17–L20.

Langer N, Norman CA, de Koter A, Vink JS, Cantiello M and Yoon SC (2007), Nov. Pair creation supernovae at low and high redshift. *A&A* 475: L19–L23. doi:10.1051/0004-6361:20078482. 0708.1970.

Laplace E, Justham S, Renzo M, Götberg Y, Farmer R, Vartanyan D and de Mink SE (2021), Dec. Different to the core: The pre-supernova structures of massive single and binary-stripped stars. *A&A* 656, A58. doi:10.1051/0004-6361/202140506. 2102.05036.

Leung SC, Nomoto K and Blinnikov S (2019), Dec. Pulsational Pair-instability Supernovae. I. Pre-collapse Evolution and Pulsational Mass Ejection. *ApJ* 887 (1), 72. doi:10.3847/1538-4357/ab4fe5. 1901.11136.

Lin W, Wang X, Yan L, Gal-Yam A, Mo J, Brink TG, Filippenko AV, Xiang D, Lunnan R, Zheng W, Brown P, Kasliwal M, Fremling C, Blagorodnova N, Mirzaqulov D, Ehgamberdiev SA, Lin H, Zhang K, Zhang J, Yan S, Zhang J, Chen Z, Deng L, Wang K, Xiao L and Wang L (2023), Jul. A superluminous supernova lightened by collisions with pulsational pair-instability shells. *Nature Astronomy* 7 (7): 779–789. ISSN 2397-3366. doi:10.1038/s41550-023-01957-3. <https://www.nature.com/articles/s41550-023-01957-3>.

Liu ZW, Röpke FK and Han Z (2023), Aug. Type Ia Supernova Explosions in Binary Systems: A Review. *Research in Astronomy and Astrophysics* 23 (8), 082001. doi:10.1088/1674-4527/acd89e. 2305.13305.

Livne E (1993), Aug. An Implicit Method for Two-dimensional Hydrodynamics. *ApJ* 412: 634. doi:10.1086/172950.

Lucy LB and Solomon PM (1970), Mar. Mass Loss by Hot Stars. *ApJ* 159: 879. doi:10.1086/150365.

Lunnan R, Chornock R, Berger E, Jones DO, Rest A, Czekala I, Dittmann J, Drout MR, Foley RJ, Fong W, Kirshner RP, Laskar T, Leibler CN, Margutti R, Milisavljevic D, Narayan G, Pan YC, Riess AG, Roth KC, Sanders NE, Scolnic D, Smartt SJ, Smith KW, Chambers KC, Draper PW, Flewelling H, Huber ME, Kaiser N, Kudritzki RP, Magnier EA, Metcalfe N, Wainscoat RJ, Waters C and Willman M (2018), Jan. Hydrogen-poor Superluminous Supernovae from the Pan-STARRS1 Medium Deep Survey. *ApJ* 852 (2), 81. doi:10.3847/1538-4357/aa9f1a. 1708.01619.

Luo Z, Barbui M, Bishop J, Chubarian G, Goldberg VZ, Harris E, Koshchiy E, Parker CE, Roosa M, Saastamoinen A, Scriven DP and Rogachev GV (2024), Feb. Radiative decay branching ratio of the Hoyle state. *PRC* 109 (2), 025801. doi:10.1103/PhysRevC.109.025801. 2310.18475.

LVK collaboration (LIGO Scientific Collaboration and Virgo Collaboration) (2016), Feb. Observation of gravitational waves from a binary black hole merger. *Phys. Rev. Lett.* 116: 061102. doi:10.1103/PhysRevLett.116.061102. <https://link.aps.org/doi/10.1103/PhysRevLett.116.061102>.

LVK collaboration (2019a), Sep. Binary Black Hole Population Properties Inferred from the First and Second Observing Runs of Advanced LIGO and Advanced Virgo. *ApJL* 882 (2), L24. doi:10.3847/2041-8213/ab3800. 1811.12940.

LVK collaboration (2019b), Jul. GWTC-1: A Gravitational-Wave Transient Catalog of Compact Binary Mergers Observed by LIGO and Virgo during the First and Second Observing Runs. *Physical Review X* 9 (3), 031040. doi:10.1103/PhysRevX.9.031040. 1811.12907.

LVK collaboration (2020a), Sep. GW190521: A Binary Black Hole Merger with a Total Mass of $150 M_{\odot}$. *PRL* 125 (10), 101102. doi:10.1103/PhysRevLett.125.101102. 2009.01075.

LVK collaboration (2020b), Jun. GW190814: Gravitational Waves from the Coalescence of a 23 Solar Mass Black Hole with a 2.6 Solar Mass Compact Object. *ApJL* 896 (2), L44. doi:10.3847/2041-8213/ab960f. 2006.12611.

LVK collaboration (2021a), Apr. GWTC-2: Compact Binary Coalescences Observed by LIGO and Virgo during the First Half of the Third Observing Run. *Physical Review X* 11 (2), 021053. doi:10.1103/PhysRevX.11.021053. 2010.14527.

LVK collaboration (2021b), May. Population Properties of Compact Objects from the Second LIGO-Virgo Gravitational-Wave Transient Catalog. *ApJL* 913 (1), L7. doi:10.3847/2041-8213/abe949. 2010.14533.

LVK collaboration (2023a), Oct. GWTC-3: Compact Binary Coalescences Observed by LIGO and Virgo during the Second Part of the Third Observing Run. *Physical Review X* 13 (4), 041039. doi:10.1103/PhysRevX.13.041039. 2111.03606.

LVK collaboration (2023b), Jan. Population of Merging Compact Binaries Inferred Using Gravitational Waves through GWTC-3. *Physical Review X* 13 (1), 011048. doi:10.1103/PhysRevX.13.011048. 2111.03634.

Maeder A and Meynet G (2000), The Evolution of Rotating Stars. *ARA&A* 38: 143. doi:10.1146/annurev.astro.38.1.143. arXiv:astro-ph/0004204.

Mapelli M, Santoliquido F, Bouffanais Y, Arca Sedda M, Giacobbo N, Artale MC and Ballone A (2020), Jul. Hierarchical mergers in young, globular and nuclear star clusters: black hole masses and merger rates. *arXiv e-prints*, arXiv:2007.15022007. 15022.

Marchant P and Moriya TJ (2020), Aug. The impact of stellar rotation on the black hole mass-gap from pair-instability supernovae. *A&A* 640, L18. doi:10.1051/0004-6361/202038902. 2007.06220.

Marchant P, Renzo M, Farmer R, Pappas KMW, Taam RE, de Mink SE and Kalogera V (2019), Sep. Pulsational Pair-instability Supernovae in Very Close Binaries. *ApJ* 882 (1), 36. doi:10.3847/1538-4357/ab3426. 1810.13412.

Mauerhan JC, Smith N, Filippenko AV, Blanchard KB, Blanchard PK, Casper CFE, Cenko SB, Clubb KI, Cohen DP, Fuller KL, Li GZ and Silverman JM (2013), Apr. The unprecedented 2012 outburst of SN 2009ip: a luminous blue variable star becomes a true supernova. *MNRAS* 430 (3): 1801–1810. doi:10.1093/mnras/stt009. 1209.6320.

Mauerhan J, Williams GG, Smith N, Smith PS, Filippenko AV, Hoffman JL, Milne P, Leonard DC, Clubb KI, Fox OD and Kelly PL (2014), Aug. Multi-epoch spectropolarimetry of SN 2009ip: direct evidence for aspherical circumstellar material. *MNRAS* 442 (2): 1166–1180. doi:10.1093/mnras/stt730. 1403.4240.

Mehta AK, Buonanno A, Gair J, Miller MC, Farag E, deBoer RJ, Wiescher M and Timmes FX (2022), Jan. Observing Intermediate-mass Black Holes and the Upper Stellar-mass gap with LIGO and Virgo. *ApJ* 924 (1), 39. doi:10.3847/1538-4357/ac3130. 2105.06366.

Miller AA, Smith N, Li W, Bloom JS, Chornock R, Filippenko AV and Prochaska JX (2010), Jun. New Observations of the Very Luminous Supernova 2006gy: Evidence for Echoes. *AJ* 139 (6): 2218–2229. doi:10.1088/0004-6256/139/6/2218. 0906.2201.

Miszuda A, Szewczuk W and Daszyńska-Daszkiewicz J (2021), Aug. The eclipsing binary systems with δ Scuti component - I. KIC 10661783. *MNRAS* 505 (3): 3206–3218. doi:10.1093/mnras/stab1597. 2105.14836.

Moe M and Di Stefano R (2017), Jun. Mind Your Ps and Qs: The Interrelation between Period (P) and Mass-ratio (Q) Distributions of Binary Stars. *ApJS* 230, 15. doi:10.3847/1538-4365/aa6fb6. 1606.05347.

Mori K, Moriya TJ, Takiwaki T, Kotake K, Horiuchi S and Blinnikov SI (2023), Jan. Light Curves and Event Rates of Axion Instability Supernovae. *ApJ* 943 (1), 12. doi:10.3847/1538-4357/acaaff. 2209.03517.

Moriya T, Tominaga N, Tanaka M, Maeda K and Nomoto K (2010), Jul. A Core-collapse Supernova Model for the Extremely Luminous Type Ic Supernova 2007bi: An Alternative to the Pair-instability Supernova Model. *ApJL* 717 (2): L83–L86. doi:10.1088/2041-8205/717/2/L83. 1004.2967.

Moriya TJ, Mazzali PA and Tanaka M (2019), Apr. Synthetic spectra of energetic core-collapse supernovae and the early spectra of SN 2007bi and SN 1999as. *MNRAS* 484 (3): 3443–3450. doi:10.1093/mnras/stz262. 1901.07628.

Moriya TJ, Inserra C, Tanaka M, Cappellaro E, Della Valle M, Hook I, Kotak R, Longo G, Mannucci F, Mattila S, Tao C, Altieri B, Amara A, Auricchio N, Bonino D, Branchini E, Brescia M, Brinchmann J, Camera S, Capobianco V, Carbone C, Carretero J, Castellano M, Cavuoti S, Cimatti A, Cledassou R, Congedo G, Conselice CJ, Conversi L, Copin Y, Corcione L, Courbin F, Cropper M, Da Silva A, Degaudenzi H, Douspis M, Dubath F, Duncan CAJ, Dupac X, Dusini S, Ealet A, Farrens S, Ferriol S, Frailey M, Franceschi E, Fumana M, Garilli B, Gillard W, Gillis B, Giocoli C, Grazian A, Grupp F, Haugan SVH, Holmes W, Hormuth F, Hornstrup A, Jahnke K, Kermiche S, Kiessling A, Kilbinger M, Kitching T, Kurki-Suonio H, Ligori S, Lilje PB, Lloro I, Maiorano E, Mansutti O, Marggraf O, Markovic K, Marulli F, Massey R, McCracken HJ, Melchior M, Meneghetti M, Meylan G, Moresco M, Moscardini L, Munari E, Niemi SM, Padilla C, Paltoni S, Pasian F, Pedersen K, Pettorino V, Ponchet M, Popa L, Raison F, Rhodes J, Riccio G, Rossetti E, Saglia R, Sartoris B, Schneider P, Secroun A, Seidel G, Sirignano C, Sirri G, Stanco L, Tallada-Crespi P, Taylor AN, Tereno I, Toledo-Moreo R, Torradefot F, Wang Y, Zamorani G, Zoubian J, Andreon S, Scottez V and Morris PW (2022), Oct. Euclid: Searching for pair-instability supernovae with the Deep Survey. *A&A* 666, A157. doi:10.1051/0004-6361/202243810. 2204.08727.

Moriya T, Fox OD, Quimby R, Schulze S, Villar A, Rest A, Grogin N, Gomez S, Rubin D, Siebert M, Kassin S, Regos E, Strolger L, Koekemoer A, Finkelstein S, Gezari S, Mattila S, Temim T, Shahbandeh M, Williams B, Chen TW, Hook I, Pierel J, Ouchi M and Harikane Y (2023), Jun. Roman CCS White Paper: Identifying high-redshift pair-instability supernovae by adding sparse F213 filter observations. *arXiv e-prints*, arXiv:2306.17212doi:10.48550/arXiv.2306.17212. 2306.17212.

Nagae C, Umeda H, Takahashi K, Yoshida T and Sumiyoshi K (2022), 09. Stability analysis of supermassive primordial stars: a new mass range for general relativistic instability supernovae. *Monthly Notices of the Royal Astronomical Society* 517 (2): 1584–1600. ISSN 0035-8711. doi:10.1093/mnras/stac2495. <https://academic.oup.com/mnras/article-pdf/517/2/1584/46454656/stac2495.pdf>, <https://doi.org/10.1093/mnras/stac2495>.

Offner SSR, Moe M, Kratter KM, Sadavoy SI, Jensen ELN and Tobin JJ (2023), Jul., The Origin and Evolution of Multiple Star Systems, Inutsuka S, Aikawa Y, Muto T, Tomida K and Tamura M, (Eds.), *Protostars and Planets VII*, Astronomical Society of the Pacific Conference Series, 534,

pp. 275, 2203. 10066.

Özel F, Psaltis D, Narayan R and McClintock JE (2010), Dec. The Black Hole Mass Distribution in the Galaxy. *ApJ* 725 (2): 1918–1927. doi: 10.1088/0004-637X/725/2/1918. 1006. 2834.

Pastorello A, Smartt SJ, Mattila S, Eldridge JJ, Young D, Itagaki K, Yamaoka H, Navasardyan H, Valenti S, Pataf F, Agnoletto I, Augusteijn T, Benetti S, Cappellaro E, Boles T, Bonnet-Bidaud JM, Botticella MT, Bufano F, Cao C, Deng J, Dennefeld M, Elias-Rosa N, Harutyunyan A, Keenan FP, Iijima T, Lorenzi V, Mazzali PA, Meng X, Nakano S, Nielsen TB, Smoker JV, Stanishev V, Turatto M, Xu D and Zampieri L (2007), Jun. A giant outburst two years before the core-collapse of a massive star. *Nature* 447 (7146): 829–832. doi:10.1038/nature05825. astro-ph/0703663.

Pastorello A, Cappellaro E, Inserra C, Smartt SJ, Pignata G, Benetti S, Valenti S, Fraser M, Takáts K, Benitez S, Botticella MT, Brimacombe J, Bufano F, Cellier-Holzem F, Costado MT, Cupani G, Curtis I, Elias-Rosa N, Ergon M, Fynbo JPU, Hambach FJ, Hamuy M, Harutyunyan A, Ivarson KM, Kankare E, Martin JC, Kotak R, LaCluyze AP, Maguire K, Mattila S, Maza J, McCrum M, Miluzio M, Norgaard-Nielsen HU, Nysewander MC, Ochner P, Pan YC, Pumo ML, Reichart DE, Tan TG, Taubenberger S, Tomasella L, Turatto M and Wright D (2013), Apr. Interacting Supernovae and Supernova Impostors: SN 2009ip, is this the End? *ApJ* 767 (1), 1. doi:10.1088/0004-637X/767/1/1. 1210. 3568.

Paxton B, Bildsten L, Dotter A, Herwig F, Lesaffre P and Timmes F (2011), Jan. Modules for Experiments in Stellar Astrophysics (MESA). *ApJS* 192, 3. doi:10.1088/0067-0049/192/1/3. 1009. 1622.

Paxton B, Cantiello M, Arras P, Bildsten L, Brown EF, Dotter A, Mankovich C, Montgomery MH, Stello D, Timmes FX and Townsend R (2013), Sep. Modules for Experiments in Stellar Astrophysics (MESA): Planets, Oscillations, Rotation, and Massive Stars. *ApJS* 208, 4. doi:10.1088/0067-0049/208/1/4. 1301. 0319.

Paxton B, Marchant P, Schwab J, Bauer EB, Bildsten L, Cantiello M, Dessart L, Farmer R, Hu H, Langer N, Townsend RHD, Townsley DM and Timmes FX (2015), Sep. Modules for Experiments in Stellar Astrophysics (MESA): Binaries, Pulsations, and Explosions. *ApJS* 220, 15. doi:10.1088/0067-0049/220/1/15. 1506. 03146.

Paxton B, Schwab J, Bauer EB, Bildsten L, Blinnikov S, Duffell P, Farmer R, Goldberg JA, Marchant P, Sorokina E, Thoul A, Townsend RHD and Timmes FX (2018), Feb. Modules for Experiments in Stellar Astrophysics (MESA): Convective Boundaries, Element Diffusion, and Massive Star Explosions. *ApJS* 234, 34. doi:10.3847/1538-4365/aaa5a8. 1710. 08424.

Paxton B, Smolec R, Schwab J, Bauer EB, Bildsten L, Blinnikov S, Duffell P, Farmer R, Goldberg JA, Jermyn AS, Kanbur SM, Marchant P, Thoul A, Townsend RHD, Wolf WM, Zhang M and Timmes FX (2019), Jul. Modules for Experiments in Stellar Astrophysics (MESA): Pulsating Variable Stars, Rotation, Convective Boundaries, and Energy Conservation. *ApJS* 243 (1), 10. doi:10.3847/1538-4365/ab2241. 1903. 01426.

Poelarends AJT, Wurtz S, Tarka J, Cole Adams L and Hills ST (2017), Dec. Electron Capture Supernovae from Close Binary Systems. *ApJ* 850 (2), 197. doi:10.3847/1538-4357/aa988a. 1710. 11143.

Powell J, Müller B and Heger A (2021), May. The final core collapse of pulsational pair instability supernovae. *MNRAS* 503 (2): 2108–2122. doi:10.1093/mnras/stab614. 2101. 06889.

Price-Whelan AM, Hogg DW, Rix HW, Beaton RL, Lewis HM, Nidever DL, Almeida A, Badenes C, Barba R, Beers TC, Carlberg JK, De Lee N, Fernández-Trincado JG, Frinchaboy PM, García-Hernández DA, Green PJ, Hasselquist S, Longa-Peña P, Majewski SR, Nitschelm C, Sobeck J, Stassun KG, Stringfellow GS and Troup NW (2020), May. Close Binary Companions to APOGEE DR16 Stars: 20,000 Binary-star Systems Across the Color-Magnitude Diagram. *ApJ* 895 (1), 2. doi:10.3847/1538-4357/ab8acc. 2002. 00014.

Quataert E, Lecoanet D and Coughlin ER (2019), May. Black hole accretion discs and luminous transients in failed supernovae from non-rotating supergiants. *MNRAS* 485 (1): L83–L88. doi:10.1093/mnrasl/slz031. 1811. 12427.

Quimby RM, Aldering G, Wheeler JC, Höflich P, Akerlof CW and Rykoff ES (2007), Oct. SN 2005ap: A Most Brilliant Explosion. *ApJL* 668 (2): L99–L102. doi:10.1086/522862. 0709. 0302.

Quimby RM, Kulkarni SR, Kasliwal MM, Gal-Yam A, Arcavi I, Sullivan M, Nugent P, Thomas R, Howell DA, Nakar E, Bildsten L, Theissen C, Law NM, Dekany R, Rahmer G, Hale D, Smith R, Ofek EO, Zolkower J, Velur V, Walters R, Henning J, Bui K, McKenna D, Poznanski D, Cenko SB and Levitan D (2011), Jun. Hydrogen-poor superluminous stellar explosions. *Nature* 474 (7352): 487–489. doi:10.1038/nature10095. 0910. 0059.

Rahman N, Janka HT, Stockinger G and Woosley SE (2022), May. Pulsational pair-instability supernovae: gravitational collapse, black hole formation, and beyond. *MNRAS* 512 (3): 4503–4540. doi:10.1093/mnras/stac758. 2112. 09707.

Rakavy G and Shaviv G (1967), Jun. Instabilities in Highly Evolved Stellar Models. *ApJ* 148: 803. doi:10.1086/149204.

Ray A, Hernandez IM, Mohite S, Creighton J and Kapadia S (2023), Nov. Nonparametric Inference of the Population of Compact Binaries from Gravitational-wave Observations Using Binned Gaussian Processes. *ApJ* 957 (1), 37. doi:10.3847/1538-4357/act452. 2304. 08046.

Rego E, Vinko J and Ziegler BL (2020), May. Detecting Pair-instability Supernovae at $z \lesssim 5$ with the James Webb Space Telescope. *ApJ* 894 (2), 94. doi:10.3847/1538-4357/ab8636. 2002. 07854.

Renzo M (2019). Live fast and die young: evolution and fate of massive stars. Ph.D. thesis, University of Amsterdam. <https://dare.uva.nl/search?identifier=ee92e82a-13e8-4add-a4ce-f2d3613e42c3>.

Renzo M and Götberg Y (2021), Dec. Evolution of Accretor Stars in Massive Binaries: Broader Implications from Modeling ζ Ophiuchi. *ApJ* 923 (2), 277. doi:10.3847/1538-4357/ac29c5. 2107. 10933.

Renzo M, Ott CD, Shore SN and de Mink SE (2017), Jul. Systematic survey of the effects of wind mass loss algorithms on the evolution of single massive stars. *A&A* 603, A118. doi:10.1051/0004-6361/201730698. 1703. 09705.

Renzo M, de Mink SE, Lennon DJ, Platais I, van der Marel RP, Laplace E, Bestenlehner JM, Evans CJ, Héault-Brunet V, Justham S, de Koter A, Langer N, Najarro F, Schneider FRN and Vink JS (2019), Jan. Space astrometry of the very massive $\sim 150 M_{\odot}$ candidate runaway star VFTS682. *MNRAS* 482: L102–L106. doi:10.1093/mnrasl/sly194. 1810. 05650.

Renzo M, Cantiello M, Metzger BD and Jiang YF (2020a), Dec. The Stellar Merger Scenario for Black Holes in the Pair-instability Gap. *ApJL* 904 (2), L13. doi:10.3847/2041-8213/abc6a6. 2010. 00705.

Renzo M, Farmer R, Justham S, Götberg Y, de Mink SE, Zapartas E, Marchant P and Smith N (2020b), Aug. Predictions for the hydrogen-free ejecta of pulsational pair-instability supernovae. *A&A* 640, A56. doi:10.1051/0004-6361/202037710. 2002. 05077.

Renzo M, Farmer RJ, Justham S, de Mink SE, Götberg Y and Marchant P (2020c), Apr. Sensitivity of the lower edge of the pair-instability black hole mass gap to the treatment of time-dependent convection. *MNRAS* 493 (3): 4333–4341. doi:10.1093/mnras/staa549. 2002. 08200.

Renzo M, Hendriks DD, van Son LAC and Farmer R (2022), Feb. Pair-instability Mass Loss for Top-down Compact Object Mass Calculations. *Research Notes of the American Astronomical Society* 6 (2), 25. doi:10.3847/2515-5172/ac503e. 2201. 10519.

Renzo M, Zapartas E, Justham S, Breivik K, Lau M, Farmer R, Cantiello M and Metzger BD (2023), Jan. Rejuvenated Accretors Have Less Bound Envelopes: Impact of Roche Lobe Overflow on Subsequent Common Envelope Events. *ApJL* 942 (2), L32. doi:10.3847/2041-8213/aca4d3. 2206. 15338.

Renzo M, Goldberg JA, Grichener A, Gottlieb O and Cantiello M (2024), Jun. Progenitor Stars Calculated with Small Reaction Networks should not be Used as Initial Conditions for Core Collapse. *Research Notes of the American Astronomical Society* 8 (6), 152. doi:10.3847/2515-5172/ad530e. 2406. 02590.

Romero-Shaw I, Lasky PD, Thrane E and Bustillo JC (2020), oct. Gw190521: Orbital eccentricity and signatures of dynamical formation in a binary black hole merger signal. *The Astrophysical Journal Letters* 903 (1): L5. doi:10.3847/2041-8213/abbe26. <https://dx.doi.org/10.3847/2041-8213/abbe26>.

Sabahhit GN, Vink JS, Sander AAC and Higgins ER (2023), Sep. Very massive stars and pair-instability supernovae: mass-loss framework for low metallicity. *MNRAS* 524 (1): 1529–1546. doi:10.1093/mnras/stad1888. 2306.11785.

Sakstein J, Croon D and McDermott SD (2022), May. Axion instability supernovae. *PRD* 105 (9), 095038. doi:10.1103/PhysRevD.105.095038. 2203.06160.

Salpeter EE (1955), Jan. The Luminosity Function and Stellar Evolution. *ApJ* 121: 161. doi:10.1086/145971.

Sana H, de Mink SE, de Koter A, Langer N, Evans CJ, Gieles M, Gossen E, Izzard RG, Le Bouquin JB and Schneider FRN (2012), Jul. Binary Interaction Dominates the Evolution of Massive Stars. *Science* 337: 444. doi:10.1126/science.1223344. 1207.6397.

Sartorio NS, Fialkov A, Hartwig T, Mirouh GM, Izzard RG, Magg M, Klessen RS, Glover SCO, Chen L, Tarumi Y and Hendriks DD (2023), May. Population III X-ray binaries and their impact on the early universe. *MNRAS* 521 (3): 4039–4055. doi:10.1093/mnras/stad697. 2303.03435.

Schneider FRN, Sana H, Evans CJ, Bestenlehner JM, Castro N, Fossati L, Gráfener G, Langer N, Ramírez-Agudelo OH, Sabin-Sanjulán C, Simón-Díaz S, Tramper F, Crowther PA, de Koter A, de Mink SE, Dufton PL, García M, Gieles M, Hénault-Brunet V, Herrero A, Izzard RG, Kalari V, Lennon DJ, Maíz Apellániz J, Markova N, Najarro F, Podsiadlowski P, Puls J, Taylor WD, van Loon JT, Vink JS and Norman C (2018), Jan. An excess of massive stars in the local 30 Doradus starburst. *Science* 359 (6371): 69–71. doi:10.1126/science.aan0106. 1801.03107.

Schneider FRN, Podsiadlowski P and Laplace E (2024), Mar. Pre-supernova evolution and final fate of stellar mergers and accretors of binary mass transfer. *arXiv e-prints*, arXiv:2403.03984 doi:10.48550/arXiv.2403.03984. 2403.03984.

Schulze S, Fransson C, Kozyreva A, Chen TW, Yaron O, Jerkstrand A, Gal-Yam A, Sollerman J, Yan L, Kangas T, Leloudas G, Ormand CMB, Smartt SJ, Yang Y, Nicholl M, Sarin N, Yao Y, Brink TG, Sharon A, Rossi A, Chen P, Chen Z, Cikota A, De K, Drake AJ, Filippenko AV, Fremling C, Fréour L, Fynbo JPU, Ho AYQ, Inserra C, Irani I, Kuncarayakti H, Lunnan R, Mazzali P, Ofek EO, Palazzi E, Perley DA, Pursiainen M, Rothberg B, Shingles LJ, Smith K, Taggart K, Tartaglia L, Zheng W, Anderson JP, Cassara L, Christensen E, George Djorgovski S, Galbany L, Gkinis A, Graham MJ, Gromadzki M, Groom SL, Hiramatu D, Andrew Howell D, Kasliwal MM, McCully C, Müller-Bravo TE, Paiano S, Paraskeva E, Pessi PJ, Polishook D, Rau A, Rigault M and Rusholme B (2024), Mar. 1100 days in the life of the supernova 2018ibb. The best pair-instability supernova candidate, to date. *A&A* 683, A223. doi:10.1051/0004-6361/202346555. 2305.05796.

Sharma Y, Sollerman J, Kulkarni SR, Moriya TJ, Schulze S, Barmentlo S, Fausnaugh M, Gal-Yam A, Jerkstrand A, Ahumada T, Bellm EC, Das KK, Drake A, Fremling C, Hale D, Hall S, Hinds KR, du Laz TJ, Karambelkar V, Kasliwal MM, Masci FJ, Miller AA, Nir G, Perley DA, Purdum JN, Qin YJ, Rehmetulla N, Rich RM, Riddle RL, Rodriguez AC, Rose S, Somalwar J, Wise JL, Wold A, Yan L and Yao Y (2024), may. Dramatic rebrightening of the type-changing stripped-envelope supernova sn 2023aew. *The Astrophysical Journal* 966 (2): 199. doi:10.3847/1538-4357/ad3758. <https://dx.doi.org/10.3847/1538-4357/ad3758>.

Shen Y, Guo B, deBoer RJ, Li E, Li Z, Li Y, Tang X, Pang D, Adhikari S, Basu C, Su J, Yan S, Fan Q, Liu J, Chen C, Han Z, Li X, Lian G, Ma T, Nan W, Nan W, Wang Y, Zeng S, Zhang H and Liu W (2023), Mar. New Determination of the $^{12}\text{C}(\alpha, \gamma)^{16}\text{O}$ Reaction Rate and Its Impact on the Black-hole Mass Gap. *ApJ* 945 (1), 41. doi:10.3847/1538-4357/acb7de.

Shibata M, Kiuchi K, Fujibayashi S and Sekiguchi Y (2021), Mar. Alternative possibility of GW190521: Gravitational waves from high-mass black hole-disk systems. *PRD* 103 (6), 063037. doi:10.1103/PhysRevD.103.063037. 2101.05440.

Siegel DM, Agarwal A, Barnes J, Metzger BD, Renzo M and Villar VA (2022), Dec. “Super-kilonovae” from Massive Collapsars as Signatures of Black Hole Birth in the Pair-instability Mass Gap. *ApJ* 941 (1), 100. doi:10.3847/1538-4357/ac8d04. 2111.03094.

Smith N (2014), Aug. Mass Loss: Its Effect on the Evolution and Fate of High-Mass Stars. *ARAA* 52: 487. doi:10.1146/annurev-astro-081913-040025. 1402.1237.

Smith N (2017), Interacting Supernovae: Types IIn and Ib, Alsabti AW and Murdin P, (Eds.), *Handbook of Supernovae*, pp. 403.

Smith N and Arnett WD (2014), Apr. Preparing for an Explosion: Hydrodynamic Instabilities and Turbulence in Presupernovae. *ApJ* 785 (2), 82. doi:10.1088/0004-637X/785/2/82. 1307.5035.

Smith N and McCray R (2007), Dec. Shell-shocked Diffusion Model for the Light Curve of SN 2006gy. *ApJL* 671 (1): L17–L20. doi:10.1086/524681. 0710.3428.

Smith N and Owocki SP (2006), Jul. On the Role of Continuum-driven Eruptions in the Evolution of Very Massive Stars and Population III Stars. *ApJL* 645 (1): L45–L48. doi:10.1086/506523. [astro-ph/0606174](https://arxiv.org/abs/0606174).

Smith N, Li W, Foley RJ, Wheeler JC, Pooley D, Chornock R, Filippenko AV, Silverman JM, Quimby R, Bloom JS and Hansen C (2007), Sep. SN 2006gy: Discovery of the Most Luminous Supernova Ever Recorded, Powered by the Death of an Extremely Massive Star like η Carinae. *ApJ* 666 (2): 1116–1128. doi:10.1086/519949. [astro-ph/0612617](https://arxiv.org/abs/0612617).

Smith N, Foley RJ, Bloom JS, Li W, Filippenko AV, Gavazzi R, Ghez A, Konopacky Q, Malkan MA, Marshall PJ, Pooley D, Treu T and Woo JH (2008), Oct. Late-Time Observations of SN 2006gy: Still Going Strong. *ApJ* 686 (1): 485–491. doi:10.1086/590141. 0802.1743.

Smith N, Chornock R, Silverman JM, Filippenko AV and Foley RJ (2010a), Feb. Spectral Evolution of the Extraordinary Type IIn Supernova 2006gy. *ApJ* 709 (2): 856–883. doi:10.1088/0004-637X/709/2/856. 0906.2200.

Smith N, Miller A, Li W, Filippenko AV, Silverman JM, Howard AW, Nugent P, Marcy GW, Bloom JS, Ghez AM, Lu J, Yelda S, Bernstein RA and Colucci JE (2010b), Apr. Discovery of Precursor Luminous Blue Variable Outbursts in Two Recent Optical Transients: The Fitfully Variable Missing Links UGC 2773-OT and SN 2009ip. *AJ* 139 (4): 1451–1467. doi:10.1088/0004-6256/139/4/1451. 0909.4792.

Smith N, Li W, Filippenko AV and Chornock R (2011a), Apr. Observed fractions of core-collapse supernova types and initial masses of their single and binary progenitor stars. *MNRAS* 412 (3): 1522–1538. doi:10.1111/j.1365-2966.2011.17229.x. 1006.3899.

Smith N, Li W, Silverman JM, Ganeshalingam M and Filippenko AV (2011b), Jul. Luminous blue variable eruptions and related transients: diversity of progenitors and outburst properties. *MNRAS* 415 (1): 773–810. doi:10.1111/j.1365-2966.2011.18763.x. 1010.3718.

Smith N, Mauerhan JC and Prieto JL (2014), Feb. SN 2009ip and SN 2010mc: core-collapse Type IIn supernovae arising from blue supergiants. *MNRAS* 438 (2): 1191–1207. doi:10.1093/mnras/stt2269. 1308.0112.

Smith N, Andrews JE, Milne P, Filippenko AV, Brink TG, Kelly PL, Yuk H and Jencson JE (2024), May. SN 2015da: late-time observations of a persistent superluminous Type IIn supernova with post-shock dust formation. *MNRAS* 530 (1): 405–423. doi:10.1093/mnras/stae726. 2312.00253.

Soker N (2024), Apr. Supernovae in 2023 (review): possible breakthroughs by late observations. *The Open Journal of Astrophysics* 7, 31. doi:10.33232/001c.117147. 2311.17732.

Spera M and Mapelli M (2017), Oct. Very massive stars, pair-instability supernovae and intermediate-mass black holes with the sevn code. *MNRAS* 470: 4739–4749. doi:10.1093/mnras/stx1576. 1706.06109.

Spera M, Mapelli M, Giacobbo N, Trani AA, Bressan A and Costa G (2019), May. Merging black hole binaries with the SEVN code. *MNRAS* 485 (1): 889–907. doi:10.1093/mnras/stz359. 1809.04605.

Spruit HC (2002), Jan. Dynamo action by differential rotation in a stably stratified stellar interior. *A&A* 381: 923–932. doi:10.1051/0004-6361:20011465. [astro-ph/0108207](https://arxiv.org/abs/0108207).

Stephenson FR and Green DA (2002), Jan. Historical supernovae and their remnants. *International Series in Astronomy and Astrophysics* 5.

Stevenson S, Sampson M, Powell J, Vigna-Gómez A, Neijssel CJ, Szécsi D and Mandel I (2019), Sep. The Impact of Pair-instability Mass Loss on the Binary Black Hole Mass Distribution. *ApJ* 882 (2), 121. doi:10.3847/1538-4357/ab3981. 1904.02821.

Stothers RB (1999), Apr. Criterion for the dynamical stability of a non-adiabatic spherical self-gravitating body. *MNRAS* 305: 365–372. doi:10.1046/j.j.1365-8711.1999.02444.x.

Takahashi K (2018), Aug. The Low Detection Rate of Pair-instability Supernovae and the Effect of the Core Carbon Fraction. *ApJ* 863 (2), 153. doi:10.3847/1538-4357/aad2d2. 1807.05373.

Takahashi K, Yoshida T, Umeda H, Sumiyoshi K and Yamada S (2016), Feb. Exact and approximate expressions of energy generation rates and their impact on the explosion properties of pair instability supernovae. *MNRAS* 456 (2): 1320–1331. doi:10.1093/mnras/stv2649. 1511.03040.

Talbot C and Thrane E (2018), Apr. Measuring the Binary Black Hole Mass Spectrum with an Astrophysically Motivated Parameterization. *ApJ* 856, 173. doi:10.3847/1538-4357/aab34c. 1801.02699.

Tanikawa A, Moriya TJ, Tominaga N and Yoshida N (2022), 11. Euclid detectability of pair instability supernovae in binary population synthesis models consistent with merging binary black holes. *Monthly Notices of the Royal Astronomical Society: Letters* 519 (1): L32–L38. ISSN 1745-3925. doi:10.1093/mnrasl/slac149. <https://academic.oup.com/mnrasl/article-pdf/519/1/L32/54610611/slac149.pdf>, <https://doi.org/10.1093/mnrasl/slac149>.

Thibodeaux PN, Ji AP, Cerny W, Kirby EN and Simon JD (2024), Apr. LAMOST J1010+2358 is not a Pair-Instability Supernova Relic. *arXiv e-prints*, arXiv:2404.170782404. 17078.

Truran JW and Arnett WD (1970), Apr. Nucleosynthesis in Explosive Oxygen Burning. *ApJ* 160: 181. doi:10.1086/150415.

Umeda H and Nagele C (2024), Feb. Metal-enriched Pair-instability Supernovae: Effects of Rotation. *ApJ* 961 (2), 146. doi:10.3847/1538-4357/ad140a. 2307.02692.

Umeda H, Yoshida T, Nagele C and Takahashi K (2020), Dec. Pulsational Pair-instability and the Mass Gap of Population III Black Holes: Effects of Overshooting. *ApJL* 905 (2), L21. doi:10.3847/2041-8213/abcb96. 2010.16032.

Unno W (1967), Jan. Stellar Radial Pulsation Coupled with the Convection. *Pub. Astr. Soc. Japan* 19: 140.

van Son LAC, De Mink SE, Broekgaarden FS, Renzo M, Justham S, Laplace E, Morán-Fraile J, Hendriks DD and Farmer R (2020), Jul. Polluting the Pair-instability Mass Gap for Binary Black Holes through Super-Eddington Accretion in Isolated Binaries. *ApJ* 897 (1), 100. doi:10.3847/1538-4357/ab9809. 2004.05187.

van Son LAC, de Mink SE, Callister T, Justham S, Renzo M, Wagg T, Broekgaarden FS, Kummer F, Pakmor R and Mandel I (2022), May. The Redshift Evolution of the Binary Black Hole Merger Rate: A Weighty Matter. *ApJ* 931 (1), 17. doi:10.3847/1538-4357/ac64a3. 2110.01634.

Vigna-Gómez A, Justham S, Mandel I, de Mink SE and Podsiadlowski P (2019), May. Massive Stellar Mergers as Precursors of Hydrogen-rich Pulsational Pair Instability Supernovae. *ApJL* 876, L29. doi:10.3847/2041-8213/ab1bdf. 1903.02135.

Vink JS (2015). Very Massive Stars in the local Universe, Springer International Publishing.

Vink JS, Higgins ER, Sander AAC and Sabhahit GN (2021), Jun. Maximum black hole mass across cosmic time. *MNRAS* 504 (1): 146–154. doi:10.1093/mnras/stab842. 2010.11730.

Wagg T, Johnston C, Bellinger EP, Renzo M, Townsend R and de Mink SE (2024), Mar. The Asteroseismic Imprints of Mass Transfer: A Case Study of a Binary Mass Gainer in the SPB Instability Strip. *arXiv e-prints*, arXiv:2403.05627doi:10.48550/arXiv.2403.05627. 2403.05627.

Wang LJ, Liu LD, Lin WL, Wang XF, Dai ZG, Li B and Song LM (2022), jul. ipft14hls in the circumstellar medium interaction model: A promising candidate for a pulsational pair-instability supernova. *The Astrophysical Journal* 933 (1): 102. doi:10.3847/1538-4357/ac7564. <https://dx.doi.org/10.3847/1538-4357/ac7564>.

Weaver TA, Zimmerman GB and Woosley SE (1978), Nov. Presupernova evolution of massive stars. *ApJ* 225: 1021–1029. doi:10.1086/156569.

Whalen DJ, Johnson JL, Smidt J, Heger A, Even W and Fryer CL (2013), Nov. The Biggest Explosions in the Universe. II. *ApJ* 777 (2), 99. doi:10.1088/0004-637X/777/2/99. 1308.3278.

Winch ERJ, Vink JS, Higgins ER and Sabhahit GN (2024), Apr. Predicting the heaviest black holes below the pair instability gap. *MNRAS* 529 (3): 2980–3002. doi:10.1093/mnras/stac393. 2401.17327.

Woosley SE (2010), Aug. Bright Supernovae from Magnetar Birth. *ApJL* 719 (2): L204–L207. doi:10.1088/2041-8205/719/2/L204. 0911.0698.

Woosley SE (2017), Feb. Pulsational Pair-instability Supernovae. *ApJ* 836, 244. doi:10.3847/1538-4357/836/2/244. 1608.08939.

Woosley SE (2019), Jun. The Evolution of Massive Helium Stars, Including Mass Loss. *ApJ* 878 (1), 49. doi:10.3847/1538-4357/ab1b41. 1901.00215.

Woosley SE and Heger A (2021), May. The Pair-instability Mass Gap for Black Holes. *ApJL* 912 (2), L31. doi:10.3847/2041-8213/abf2c4. 2103.07933.

Woosley SE and Smith N (2022), Oct. SN 1961V: A Pulsational Pair-instability Supernova. *ApJ* 938 (1), 57. doi:10.3847/1538-4357/ac8eb3. 2205.06386.

Woosley SE, Heger A and Weaver TA (2002), Nov. The evolution and explosion of massive stars. *Rev. Mod. Phys.* 74: 1015. doi:10.1103/RevModPhys.74.1015.

Woosley SE, Blinnikov S and Heger A (2007), Nov. Pulsational pair instability as an explanation for the most luminous supernovae. *Nature* 450: 390–392. doi:10.1038/nature06333. 0710.3314.

Wyrzykowski Ł and Mandel I (2020), Apr. Constraining the masses of microlensing black holes and the mass gap with Gaia DR2. *A&A* 636, A20. doi:10.1051/0004-6361/201935842. 1904.07789.

Xi Z (1955). A New Catalogue of Ancient Novae. *Acta Astronomica Sinica* 3: 183–196.

Xing QF, Zhao G, Liu ZW, Heger A, Han ZW, Aoki W, Chen YQ, Ishigaki MN, Li HN and Zhao JK (2023), Jun. A metal-poor star with abundances from a pair-instability supernova. *Nature* 618 (7966): 712–715. doi:10.1038/s41586-023-06028-1.

Yamada S (1997), Feb. An Implicit Lagrangian Code for Spherically Symmetric General Relativistic Hydrodynamics with an Approximate Riemann Solver. *ApJ* 475 (2): 720–739. doi:10.1086/303548. astro-ph/9601042.

Yoshida T, Umeda H, Maeda K and Ishii T (2016), Mar. Mass ejection by pulsational pair instability in very massive stars and implications for luminous supernovae. *MNRAS* 457: 351–361. doi:10.1093/mnras/stv3002. 1511.01695.

Yusof N, Hirschi R, Meynet G, Crowther PA, Ekström S, Frischknecht U, Georgy C, Abu Kassim H and Schnurr O (2013), Aug. Evolution and fate of very massive stars. *MNRAS* 433 (2): 1114–1132. doi:10.1093/mnras/stt794. 1305.2099.

Yusof N, Hirschi R, Eggenberger P, Ekström S, Georgy C, Sibony Y, Crowther PA, Meynet G, Kassim HA, Harun WAW, Maeder A, Groh JH, Farrell E and Murphy L (2022), Apr. Grids of stellar models with rotation VII: models from 0.8 to 300 M_⊙ at supersolar metallicity (Z = 0.020). *MNRAS* 511 (2): 2814–2828. doi:10.1093/mnras/stac230. 2201.08645.

Zapartas E, de Mink SE, Justham S, Smith N, Renzo M and de Koter A (2021), Jan. Effect of binary evolution on the inferred initial and final core masses of hydrogen-rich, Type II supernova progenitors. *A&A* 645, A6. doi:10.1051/0004-6361/202037744. 2002.07230.

Zeldovich YB and Novikov ID (1999). Stars and relativity.

Zhou P, Vink J, Li G and Domček V (2018), Sep. G7.7-3.7: A Young Supernova Remnant Probably Associated with the Guest Star in 386 CE

(SN 386). *ApJL* 865, L6. doi:10.3847/2041-8213/aae07d. 1809.03535.

Ziegler J and Freese K (2021), Aug. Filling the black hole mass gap: Avoiding pair instability in massive stars through addition of nonnuclear energy. *PRD* 104 (4), 043015. doi:10.1103/PhysRevD.104.043015. 2010.00254.

Zinnecker H and Yorke HW (2007), Sep. Toward Understanding Massive Star Formation. *ARAA* 45 (1): 481–563. doi:10.1146/annurev.astro.44.051905.092549. 0707.1279.

Zwicky F (1964), Feb. NGC 1058 and its Supernova 1961. *ApJ* 139: 514. doi:10.1086/147779.